Article

Cell

Derivation of Pluripotent Stem Cells with In Vivo Embryonic and Extraembryonic Potency

Graphical Abstract

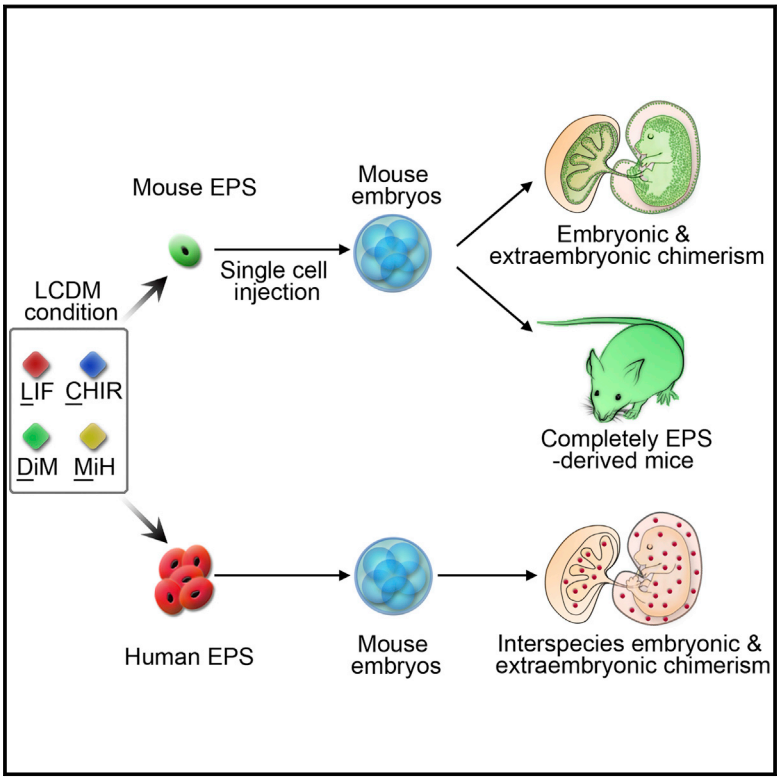

Authors

Yang Yang, Bei Liu, Jun Xu, ..., Huan Shen, Juan Carlos Izpisua Belmonte, Hongkui Deng

Correspondence

rmivf@sina.com (H.S.), belmonte@salk.edu (J.C.I.B.), hongkui_deng@pku.edu.cn (H.D.)

In Brief

Pluripotent stem cells in a defined chemical culture condition can generate both embryonic and extraembryonic tissues at the single-cell level.

Highlights

- A chemical cocktail enables derivation of EPS cells from both humans and mice
- A single mouse EPS cell generates both embryonic and extraembryonic lineages in vivo
- Mouse EPS cells show robust and superior chimeric ability at the single cell level
- Human EPS cells show interspecies chimeric competency in mouse conceptuses

Data Resources

GSE89303
GSE80732
GSE89301

Yang et al., 2017, Cell *169*, 243–257
April 6, 2017
http://dx.doi.org/10.1016/j.cell.2017.02.005

CellPress

Cell

Derivation of Pluripotent Stem Cells with In Vivo Embryonic and Extraembryonic Potency

Yang Yang,[1,2,15] Bei Liu,[1,2,15] Jun Xu,[1,15] Jinlin Wang,[1,15] Jun Wu,[3,15] Cheng Shi,[4] Yaxing Xu,[5] Jiebin Dong,[1] Chengyan Wang,[1] Weifeng Lai,[5] Jialiang Zhu,[1] Liang Xiong,[5] Dicong Zhu,[1,2] Xiang Li,[1] Weifeng Yang,[6] Takayoshi Yamauchi,[3] Atsushi Sugawara,[3] Zhongwei Li,[3] Fangyuan Sun,[7] Xiangyun Li,[7] Chen Li,[8] Aibin He,[8] Yaqin Du,[1] Ting Wang,[1] Chaoran Zhao,[1] Haibo Li,[1] Xiaochun Chi,[9] Hongquan Zhang,[9] Yifang Liu,[10] Cheng Li,[11,12,13] Shuguang Duo,[14] Ming Yin,[6] Huan Shen,[4,*] Juan Carlos Izpisua Belmonte,[3,*] and Hongkui Deng[1,2,16,*]

[1]Department of Cell Biology, School of Basic Medical Sciences, Peking University Stem Cell Research Center, State Key Laboratory of Natural and Biomimetic Drugs, Peking University Health Science Center and the MOE Key Laboratory of Cell Proliferation and Differentiation, College of Life Sciences, Peking-Tsinghua Center for Life Sciences, Peking University, Beijing 100191, China

[2]Shenzhen Stem Cell Engineering Laboratory, Key Laboratory of Chemical Genomics, Peking University Shenzhen Graduate School, Shenzhen 518055, China

[3]Gene Expression Laboratory, The Salk Institute for Biological Studies, 10010 N. Torrey Pines Rd., La Jolla, CA 92037, USA

[4]Reproductive Medical Center, Peking University People's Hospital, Peking University, Beijing, 100044, China

[5]Peking University-Tsinghua University-National Institute of Biological Sciences Joint Graduate Program, College of Life Sciences, Peking University, Beijing 100871, China

[6]Beijing Vitalstar Biotechnology, Beijing 100012, China

[7]College of Animal Science and Technology, Hebei University, Baoding 071002, China

[8]Institute of Molecular Medicine, Peking University, PKU-Tsinghua U Joint Center for Life Sciences, Beijing 100871, China

[9]Laboratory of Stem Cells, Development and Reproductive Medicine, Department of Anatomy, Histology and Embryology, School of Basic Medical Sciences, Peking University, Beijing 100191, China

[10]School of Life Sciences, Tsinghua University, Beijing 100084, China

[11]Peking-Tsinghua Center for Life Sciences, Academy for Advanced Interdisciplinary Studies

[12]School of Life Sciences, Center for Statistical Science

[13]Center for Bioinformatics

Peking University, Beijing 100871, China

[14]Institute of Zoology, Chinese Academy Sciences, Beijing 100101, China

[15]These authors contributed equally

[16]Lead Contact

*Correspondence: rmivf@sina.com (H.S.), belmonte@salk.edu (J.C.I.B.), hongkui_deng@pku.edu.cn (H.D.)

http://dx.doi.org/10.1016/j.cell.2017.02.005

SUMMARY

Of all known cultured stem cell types, pluripotent stem cells (PSCs) sit atop the landscape of developmental potency and are characterized by their ability to generate all cell types of an adult organism. However, PSCs show limited contribution to the extraembryonic placental tissues in vivo. Here, we show that a chemical cocktail enables the derivation of stem cells with unique functional and molecular features from mice and humans, designated as extended pluripotent stem (EPS) cells, which are capable of chimerizing both embryonic and extraembryonic tissues. Notably, a single mouse EPS cell shows widespread chimeric contribution to both embryonic and extraembryonic lineages in vivo and permits generating single-EPS-cell-derived mice by tetraploid complementation. Furthermore, human EPS cells exhibit interspecies chimeric competency in mouse conceptuses. Our findings constitute a first step toward capturing pluripotent stem cells with extraembryonic developmental potentials in culture and open new avenues for basic and translational research.

INTRODUCTION

Of all known types of in vitro derived stem cells, pluripotent stem cells (PSCs) are regarded to harbor the greatest developmental potency and can generate all the cell types of an adult organism (Evans and Kaufman, 1981; Martin, 1981; Thomson et al., 1998). The derivation of PSCs with distinct molecular and functional properties led to the realization that different phases of pluripotency, e.g., naive and primed, could be stabilized in vitro with different culture parameters (Brons et al., 2007; Nichols and Smith, 2009; Tesar et al., 2007; Wu et al., 2015). Compared to primed PSCs, naive PSCs presumably harbor higher developmental potential, which have been derived in mice (Ying et al., 2008), rats (Buehr et al., 2008; Li et al., 2008), humans (Chan et al., 2013; Gafni et al., 2013; Guo et al., 2016; Takashima et al., 2014; Theunissen et al., 2014; Wang et al., 2014; Ware et al., 2014), and non-human primates (Chen et al., 2015; Fang et al., 2014). Notwithstanding their ample developmental potency toward all embryonic (Em) derivatives, however, PSCs are limited in their ability to contribute to

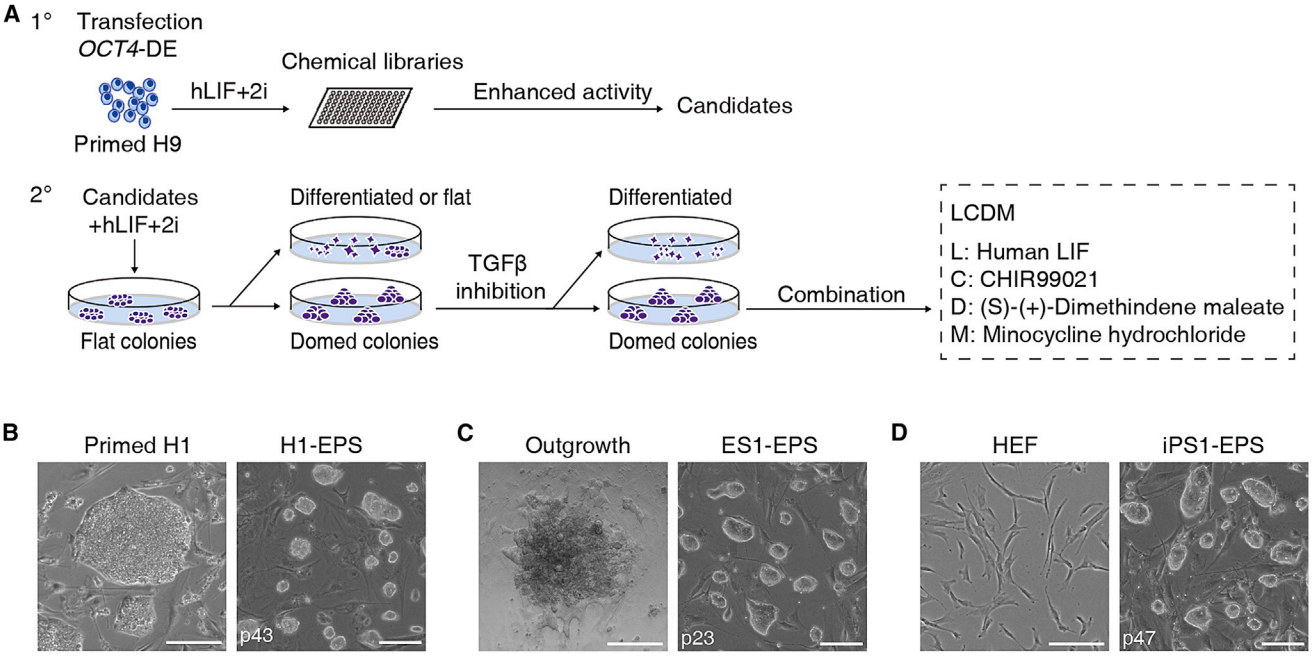

Figure 1. Identification of a Chemical Cocktail that Supports hEPS Cell Generation

(A) Strategies used for screening compounds.

(B–D) Representative images showing the generation of hEPS cells by conversion of primed hPSCs (B), by de novo derivation from human blastocysts (C), or by somatic reprogramming (D). Scale bars, 100 μm.

See also Figure S1.

extraembryonic (ExEm) tissues, in particular, to the trophoblast lineages that contribute to placental development (Beddington and Robertson, 1989).

During pre-implantation development, both the zygote and blastomeres are considered totipotent, given that they can give rise to all Em and ExEm lineages (Papaioannou et al., 1989; Tarkowski, 1959). Upon being fated to inner cell mass (ICM) or trophectoderm (TE), the developmental potency of embryonic cells becomes more restricted. Additional cell divisions lead to the formation of three lineages in a mature blastocyst—epiblast, primitive endoderm, and TE—and their developmental potencies have been captured in vitro by the derivation of embryonic stem (ES) cells (Evans and Kaufman, 1981; Martin, 1981), ExEm endoderm cells (Kunath et al., 2005), and trophoblast stem (TS) cells (Tanaka et al., 1998), respectively. The ability to culture all three lineages of a blastocyst begs the question of whether a cellular state with bi-potential toward both Em and ExEm lineages can be stabilized in vitro.

Recent studies have identified subpopulations of cells within mouse ES cell cultures that can contribute to both Em and ExEm lineages (Macfarlan et al., 2012; Morgani et al., 2013). Interestingly, in vivo reprograming also generated transient cells with similar features (Abad et al., 2013). These cells, however, could not be stably maintained in culture nor were they rigorously tested for their developmental potential in vivo. Therefore, it remains unresolved whether it is feasible to derive and maintain stable mammalian stem cell lines with greater developmental potency than PSCs.

In this study, through chemical screening, we have identified a chemical cocktail conferring both embryonic and ExEm chimeric competency to both human and mouse PSCs. These cells, designated as extended pluripotent stem (EPS) cells, can be derived from blastocysts, converted from known PSCs, as well as generated by somatic reprogramming. EPS cells can be stably maintained long term in culture while retaining the ability to contribute, at single-cell level, to both Em and ExEm lineages.

RESULTS

Identification of a Chemical Cocktail that Supports the Generation of Human PSCs with Mouse ES Cell Features

We initially focused on identifying conditions that support human naive pluripotency. According to the mouse ground state condition (PD 0325901, CHIR 99021, and human LIF [hLIF]), we screened additional chemical compounds that could activate the *OCT4* distal enhancer (*OCT4*-DE), which drives *OCT4* expression in preimplantation embryos and also serves as a molecular marker of naive pluripotency (Tesar et al., 2007; Yeom et al., 1996) in primed human H9 ES cells (Figure 1A and Table S1). More than 100 primary hits were further screened in order to identify candidates that relieve human PSCs (hPSCs) from transforming growth factor (TGF)-β-signaling dependency, an indispensable pathway for primed hPSC self-renewal (Vallier et al., 2005). More than 30 small molecules were identified after the screening, which supported dome-shaped hPSC colony formation, a morphological feature characteristic of naive

pluripotent cells. Different combinations of these small molecules were further tested to identify candidates that could support long-term self-renewal of these colonies. Two small molecules, (S)-(+)-dimethindene maleate (DiM) and minocycline hydrochloride (MiH), were identified. In addition, we found that MEK inhibition was dispensable for the maintenance of dome-shaped colonies, and long-term treatment of TGFβ inhibitor impaired the self-renewal of these colonies (data not shown). After optimization, we established a minimal condition consisting of hLIF, CHIR 99021, DiM, and MiH (LCDM), which supported the conversion and long-term maintenance of dome-shaped hPSCs from primed hPSCs (Figures 1A and 1B and S1A). Additionally, we found that this condition also enabled de novo derivation of ES cells from human blastocysts (Figure 1C) and human-induced pluripotent stem cells (hiPSCs) from fibroblasts (Figure 1D). LCDM-hPSCs grew faster than primed hPSCs (Figure S1B), showed high single-cell cloning efficiency (Figure S1C), expressed pluripotency markers (Figure S1D), and showed the ability to differentiate into the three embryonic germ layers (Figures S1E and S1F and Table S2). Furthermore, they showed several features of naive mouse ES (mES) cells, including increased *OCT4*-DE activity (Figure S1G) and absence of foci of histone 3 lysine 27 trimethylation (H3K27me3) in female cell lines (Figure S1H). In addition, LCDM-hPSCs showed genome stability after more than 50 passages (Figures S1I and S1J and Table S2). In addition to supporting derivation and conversion in humans, the LCDM condition also supported de novo ES cell derivation from mouse blastocysts (Figure 2A and Table S2) and conversion from mES cells (Figure 2B and Table S2). LCDM-mES cells expressed pluripotency marker genes (Figure S2A), generated all three embryonic germ layers (Figures S2B and S2C), and maintained a normal karyotype (Figure S2D). Further analysis showed that LCDM-mES cells also generated chimeras with germline transmission (Figure S2E) and permitted mouse generation through tetraploid complementation (Figures S2F and S2G). Collectively, these results indicate that the LCDM condition supports the generation of human and mouse PSCs with features resembling those of mES cells.

Em and ExEm Developmental Potency of Mouse EPS Cells

While examining the in vivo developmental potential of LCDM-mES cells by using the chimera assay, we noticed the integration of LCDM-mES-derived cells into ExEm tissues, in addition to the Em tissues, including the placenta and yolk sac (24/60 recovered embryonic day (E)12.5 conceptuses) (Figures 2C and 2D). This is in contrast to mES cells that showed embryonic chimerism (31/78 recovered embryos) (Figures 2C and 2D) and the ability to integrate into the yolk sac but were not able to efficiently contribute to the placenta, as judged by direct observation of reporter fluorescence (0/78 recovered conceptuses), results consistent with a previous report (Beddington and Robertson, 1989). These results suggest that LCDM-mES cells may have acquired an extended developmental potency toward ExEm lineages, and hereafter we designate them as EPS cells.

To unequivocally demonstrate mouse EPS (mEPS) cells' developmental potency, we employed a highly stringent assay and examined the chimera forming ability of a single donor cell. To this end, we injected a single fluorescent-labeled mEPS cell into an eight-cell (8C)-stage mouse embryo (Figure 2E) and examined its chimeric contribution after 48–60 hr of in vitro culture. Notably, 32.9% (86/261) of recovered blastocysts showed concomitant differentiation of a single mEPS cell to both the TE and ICM in chimeric blastocysts (Figure 2F and Table S3), which was evidenced by the co-expression of Tdtomato with TE markers CDX2 or GATA3 in the outer layer of blastocysts and with pluripotency markers OCT4 or NANOG in the ICM (Figure 2G). In contrast, single-mES-cell derivatives contributed only to ICM, not to both TE and ICM (0/139 recovered blastocysts) (Figure 2F and Table S3).

To functionally evaluate the blastocyst derivatives of a single mEPS cell, we next tested ES and TS cell derivation. To this end, chimeric blastocysts with contribution of single mEPS-derived cells into both TE and ICM were seeded and further passaged into mouse ES and TS cell media respectively, which supported the derivation of Tdtomato$^+$ mEPS-derived ES (EPS-ES) and TS (EPS-TS) cell colonies simultaneously (Figures 3A and 3B). We also established, as a control, a mES cell line (2i-ES) from a chimeric blastocyst developed from an 8C embryo injected with multiple Tdtomato$^+$ mES cells (Figure 3C). However, no Tdtomato$^+$ TS-like colonies could be established using blastocyst (0/48 embryos) derived from 8C embryos injected with mES cells (Figure 3C). EPS-ES cells expressed the pluripotency markers but not the TS markers (Figure S3A). EPS-ES cells only gave rise to embryonic tissue, not placenta, in chimeric conceptuses (Figure 3D). On the other hand, EPS-TS cells expressed typical TS markers but not the pluripotency markers (Figure S3B). EPS-TS cells only integrated into placental tissue in chimeric conceptuses (Figure 3E). To exclude the possibility that mEPS cells could be directly converted into TS cells in TS medium, we cultured mEPS cells in TS medium for three passages and found that TS-cultured mEPS cells did not upregulate TS markers (Figures S3C and S3D) and still maintained NANOG expression (Figure S3D). These results support the conclusion that EPS-TS cells are derived from mEPS-differentiated TE cells rather than through direct conversion. Collectively, these data demonstrate the developmental potential of a single mEPS cell toward both ICM and TE lineages during preimplantation mouse development.

We next analyzed single-mEPS-cell-derived chimeras beyond the preimplantation stage and observed the integration of single-donor mEPS cell derivatives in both Em and ExEm tissues in E10.5 (21/90 recovered conceptuses) and E12.5 (10/63 recovered conceptuses) conceptuses (Table S3). Fluorescence-activated cell sorting (FACS) analysis further confirmed the wide-spread integration of single-mEPS-cell derivatives in E10.5 embryo, yolk sac, and placenta (Figures 4A and S4A). Notably, single-mEPS-cell derivatives integrated into the trophoblast layers of the chimeric placentas and expressed the trophoblast marker CK8 (Figure 4B). These cells were also observed in the layers of trophoblast giant cells (TGCs) and spongiotrophoblast, which expressed TGC marker PLF (proliferin) and spongiotrophoblast marker TPBPA respectively (Figures 4C and 4D). Single-mEPS-cell derivatives also chimerized both the Em and ExEm tissues in the late-gestation E17.5 conceptuses (13/94 recovered conceptuses) (Figures 4E and S4B and Table S3), and the

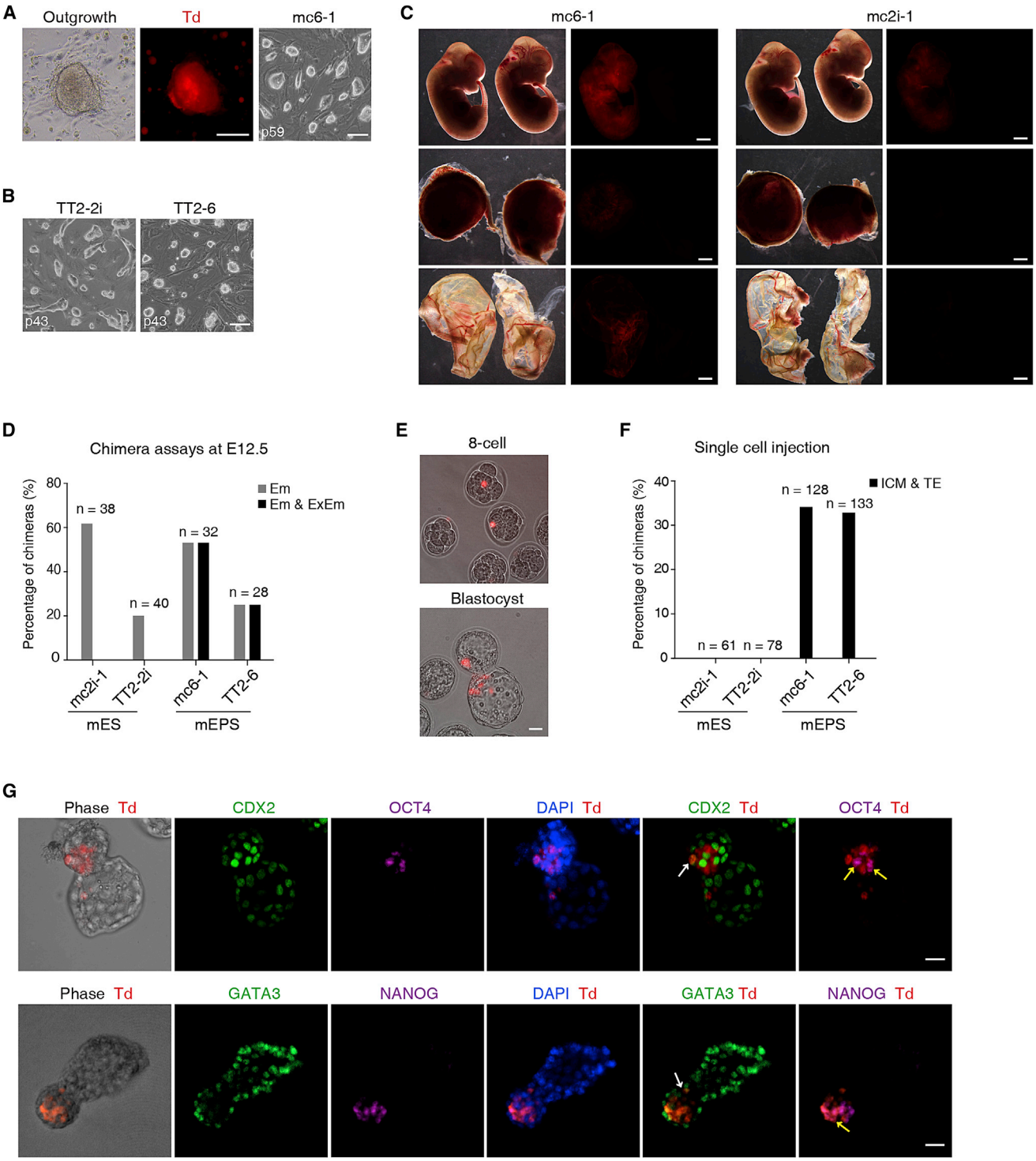

Figure 2. The LCDM Condition Can Support the Generation of mEPS Cells with Extended Developmental Potency

(A and B) Derivation of mEPS cells from blastocysts (A) and by conversion of mES cells (B). Scale bars, 100 μm. Td, Tdtomato fluorescent signal.

(C) Representative images showing the integration of mEPS-derived cells (mc6-1, Tdtomato labeled, left panels) into the embryo, placenta and yolk sac. Conventional mES cells (mc2i-1, Tdtomato labeled, right panels) contribute to the embryo and yolk sac. In each image, samples on the right side are from one un-injected conceptus. Scale bars, 1 mm.

(D) Summary of E12.5 chimera assays by multiple cell injection. The bar chart shows the percentages of chimeras (gray, integration into embryonic tissues [Em]; black, integration into both embryonic and ExEm placental tissues [Em & ExEm]) among the recovered E12.5 conceptuses. n indicates numbers of recovered E12.5 conceptuses.

(legend continued on next page)

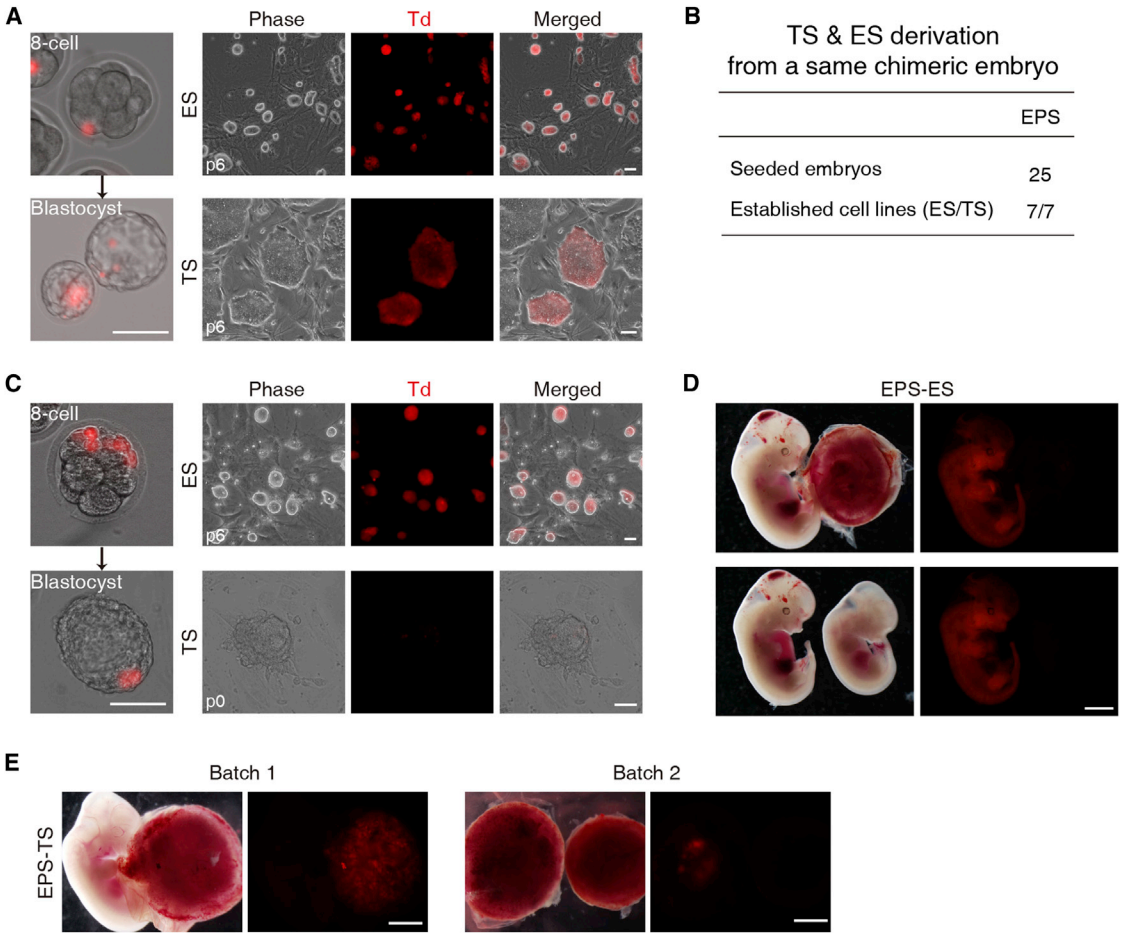

Figure 3. ES and TS Cell Derivation from a Single-mEPS-cell-derived Chimeric Blastocyst

(A) Diagrams showing the injection of single mEPS cells into 8C embryos, which were used for establishing ES and TS cells 48–60 hr later. Representative images showing the derivation of both ES (EPS-ES, upper right panels) and TS (EPS-TS, lower right panels) cells from the same single mEPS-chimerized blastocysts. Td, Tdtomato fluorescent signal. Scale bars, 100 μm.

(B) Summary of mEPS-derived ES and TS cell derivation from the same single-mEPS-chimerized embryos.

(C) Diagrams showing the injection of multiple mES cells into 8C embryos, which were used for establishing ES and TS cells 48–60 hr later. Representative images showing the derivation of ES (2i-ES) but not TS cells from multiple mES-chimerized blastocysts. Td, Tdtomato fluorescent signal. Scale bars, 100 μm.

(D) Representative images showing EPS-ES cells can integrate into E13.5 embryos but not placenta. Scale bar, 1 mm. In the lower panels, the embryo on the right side is from one un-injected conceptus.

(E) Representative images showing EPS-TS cells can only integrate into placenta of E13.5 mouse conceptuses. In the right panels, the placentas on the right side are from an un-injected conceptus. Scale bars, 1 mm.

See also Figure S3.

percentage that a single-mEPS-cell derivative contributed to the E17.5 chimeric placentas could be up to 19% (Figure S4C). To further evaluate the functionality of single-EPS-cell-derived trophoblasts, we tested their invasive ability by using the Transwell-based invasive assay (Figure S4D), which is one of the most prominent functional features of trophoblasts. Tdtomato$^+$ single-mEPS-cell-derived placental cells, which expressed the trophoblast markers CK8 and CK7, were able to migrate through the membrane pores (Figure S4E), highlighting their invasive nature. On the other hand, the mRNA expression of multiple

(E) Diagrams showing the injection of a single Tdtomato-labeled mEPS cell into an 8C-stage embryo, which was analyzed 48–60 hr later. Scale bar, 20 μm.

(F) Summary of chimeric assays of single-cell injection at the 8C embryo stage. The bar chart shows the percentage of chimeras among the recovered blastocysts. ICM & TE, embryos with the integration of mouse cells into both ICM and TE. n indicates numbers of recovered blastocysts.

(G) Representative images showing immunostaining of single mEPS-derived chimeric blastocysts with antibodies specific to ICM and TE markers. Td, direct observation of Tdtomato fluorescent signal. White arrow, Tdtomato$^+$/CDX2$^+$ cells (in the upper image) or Tdtomato$^+$/GATA3$^+$ cells (in the lower image); yellow arrows, Tdtomato$^+$/OCT4$^+$ cells (in the upper image) or Tdtomato$^+$/NANOG$^+$ cells (in the lower image). Scale bars, 20 μm.

See also Figure S2.

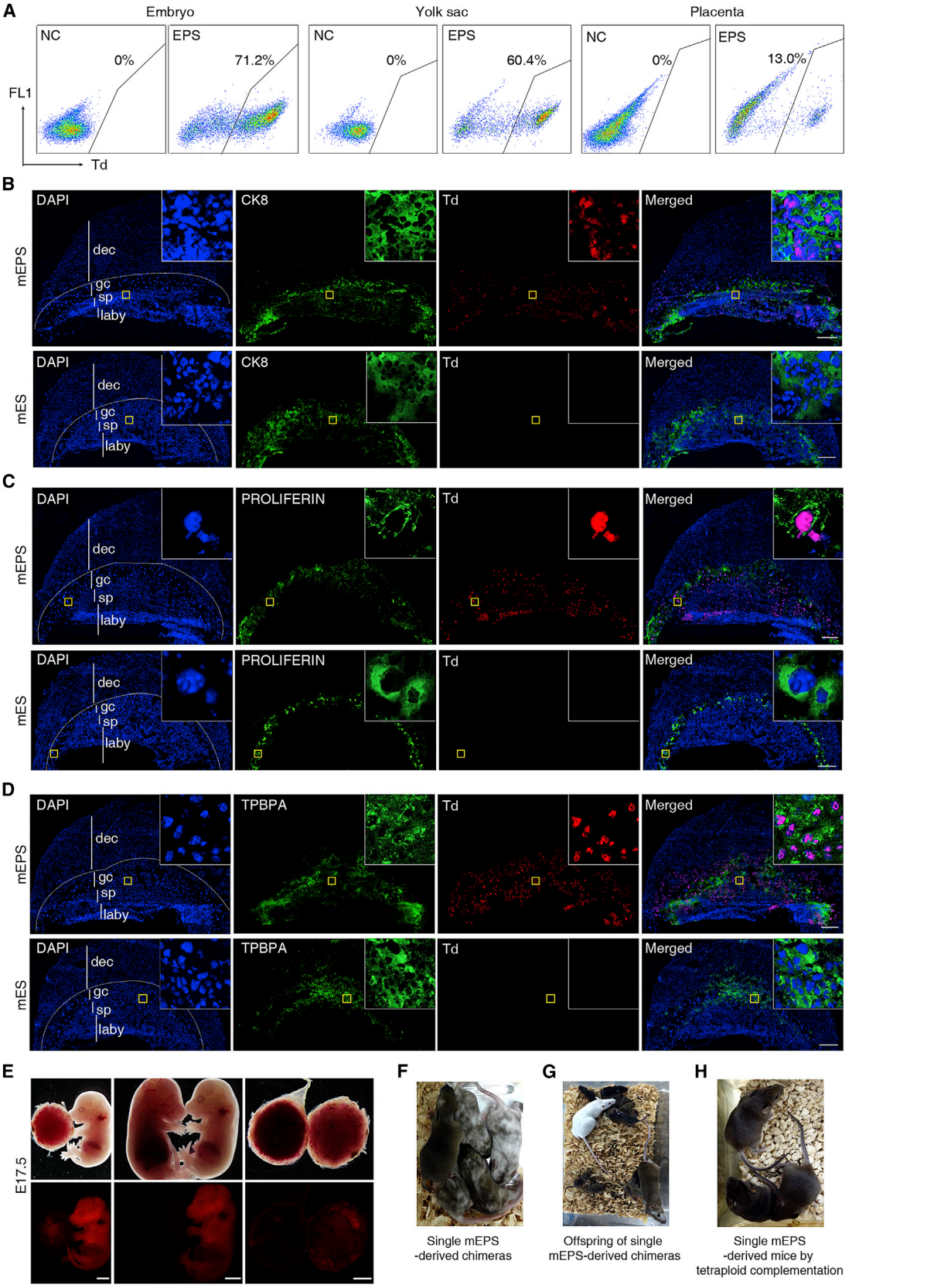

(legend on next page)

trophoblast markers, such as *Hand1*, *Plf*, *Pl2*, and *Tpbp-α*, were significantly upregulated in mEPS-cell-derived placental cells when compared to original mEPS cells (Figure S4F). Moreover, FACS analysis revealed the presence of polyploid cells in mEPS-cell-derived placental cells, implying endoreduplication of mEPS-cell-derived trophoblasts (Figure S4G).

We further tested whether it is possible to obtain single-mEPS-cell-derived postnatal chimeric mice. Of all 113 born pups, 59 single-mEPS-cell-derived chimeras (52.2%) were obtained (Figure 4F and Table S3). Furthermore, these single-mEPS-cell-derived chimeras showed robust germline competency (87.8%, 36 out of 41 chimeric mice tested) (Figures 4G and Table S3). Finally, we examined the developmental potency of single mEPS cells by tetraploid complementation. Importantly, single mEPS cells could produce completely EPS-cell-derived mice by tetraploid complementation (7 mice/311 injected blastocysts) (Figures 4H and S4H and S4I). Taken together, these data demonstrate the bona fide pluripotency of EPS cells and their chimeric competency to both Em and ExEm lineages at the single-cell level.

Interspecies Chimeric Competency of Human EPS cells

The chimera forming ability of mEPS cells led us to examine whether human EPS (hEPS) cells could also generate interspecies human-mouse conceptuses. We injected a single fluorescent-labeled hEPS cell into an 8C-stage mouse embryo (Figure 5A) and examined its chimeric contribution after 48–60 hr of in vitro culture by co-staining with TE and ICM markers. Our results showed concomitant differentiation of a single hEPS cell into cells expressing TE or ICM markers, respectively (51/345 recovered embryos, 14.7%), in chimeric blastocysts (Figures 5B and 5C and S5 and Table S4). As the control, primed hPSCs could not form chimeric blastocysts after single-cell injection (0/143 recovered embryos) (Figures 5B and 5C and S5 and Table S4), which is consistent with previously reported poor chimerism of primate primed PSCs in preimplantation embryos (Gafni et al., 2013; James et al., 2006; Tachibana et al., 2012).

We next examined the chimeric competency of hEPS cells in post-implantation mouse conceptuses. The presence of human cells in mouse E10.5 conceptuses was identified by immunostaining with the anti-human nuclei (hN) antibody or by detection of fluorescent proteins from fluorescent-labeled hEPS cells. Interspecies chimerism was observed in E10.5 embryos with hEPS cells (Figures S6A and S6C), but not with primed hPSCs (Figure S6A) or un-injected controls (data not shown). Intriguingly, we also observed the integration of hEPS-cell derivatives into ExEm tissues such as the placenta and yolk sac (Figure S6B and S6D). In contrast, we did not observe the presence of human cells in the mouse placenta injected with primed hPSCs (Figure S6B).

To further confirm the interspecies chimerism of hEPS cells, we employed a highly sensitive mitochondrial PCR assay to quantitatively analyze the degree of integration of hEPS cells in mouse conceptuses (Cohen et al., 2016; Theunissen et al., 2016). Notably, 34.4% of recovered hEPS-cell-derived mouse embryos (41/119 recovered embryos) contained human cells (we used 1 human cell in 10,000 mouse cells as the threshold). The percentage of human cells varied and in some cases reached 1% (Figure S6E and Table S4). In addition, 18.0% of recovered hEPS-derived mouse placentas (24/133 recovered placentas) showed human cell contribution (Figure S6F and Table S4), the percentage of which could reach more than 0.1%. Among 54 analyzed mouse conceptuses, six (11.1%) showed dual integration of hEPS-cell derivatives to both mouse embryos and placentas (Table S4). As a control, primed hPSCs showed no integration in mouse embryo or placenta (0/54 analyzed mouse conceptuses) (Table S4). Compared to mEPS cells, the percentage of hEPS cell chimerism in mouse conceptuses is still limited and varied between different batches, which in part can be attributed to species-specific development differences between humans and mice (Rossant and Tam, 2017). Although these results further confirm the presence of hEPS-cell derivatives in mouse conceptuses, it should be noted that the mitochondrial PCR assay can neither ascertain whether detected human cells are alive nor enable analysis of their lineage identities.

We next attempted to investigate the fate of hEPS-cell derivatives in chimeric mouse conceptuses. In E6.5–E7.5 chimeric mouse conceptuses, using human specific primers, we detected the mRNA expression of several human lineage markers by RT-PCR, including *PAX6*, *FOXA2*, *SOX17*, *T*, *GATA6*, and *CK8* (Figure S6G). In E10.5 chimeric embryos, hEPS-cell derivatives lost expression of the pluripotency marker NANOG (Figure S6H). We further examined the identity of these cells by immunostaining with different lineage markers. In several chimeric embryos, we found that hN^+ cells co-expressed appropriate lineage-specific markers such as SOX2 and GATA4 (Figures 6A and 6B). In addition, hEPS-derived cells residing in the trophoblast layers expressed the trophoblast marker CK8 (Figure 6C). It is also notable that weak signals of hCG-β immunostaining could be detected in several samples (data not shown), which could also be

Figure 4. Single mEPS-Derived Cells Can Contribute To Both Embryonic and Extraembryonic Lineages In Vivo

(A) Representative FACS analysis of the percentages of single-mEPS-cell derivations (Td, Tdtomato labeled) from the same E10.5 conceptus. NC, samples isolated from an un-injected mouse E10.5 conceptus.

(B–D) Representative whole-placenta confocal images showing single mEPS-derived cells (Tdtomato labeled) can contribute to trophoblastic lineages in chimeric E10.5 placentas. Single mES cells were injected as controls. The placentas were stained with anti-CK8 (B), anti-PROLIFERIN (C), and anti-TPBPA (D) antibodies. Td, direct observation of Tdtomato fluorescent signal; dec, decidua layer; gc, giant cell layer; sp, spongiotrophoblast layer; laby, labyrinth layer. The insets are enlargements of the yellow boxes. The pseudo-colors were used. Scale bars, 200 μm.

(E) Representative images showing contribution of single mEPS-derived cells (Tdtomato labeled) into both embryo and placenta in E17.5 mouse conceptuses. Images for single mEPS-chimerized placentas shown in the left and right panels are taken from the same placental sample from different sides (front side in the left panel, back side in the right panel). For middle and right panels, samples on the left side in each image are from one un-injected conceptus. Scale bars, 2.5 mm.

(F and G) Representative images showing single mEPS-derived chimeras (C1-EPS 19#) (F) and germline transmission of single mEPS cells (G). See also Table S3.

(H) A representative image of single mEPS cell-derived mice (C1-EPS 12#) through tetraploid complementation.

See also Figure S4.

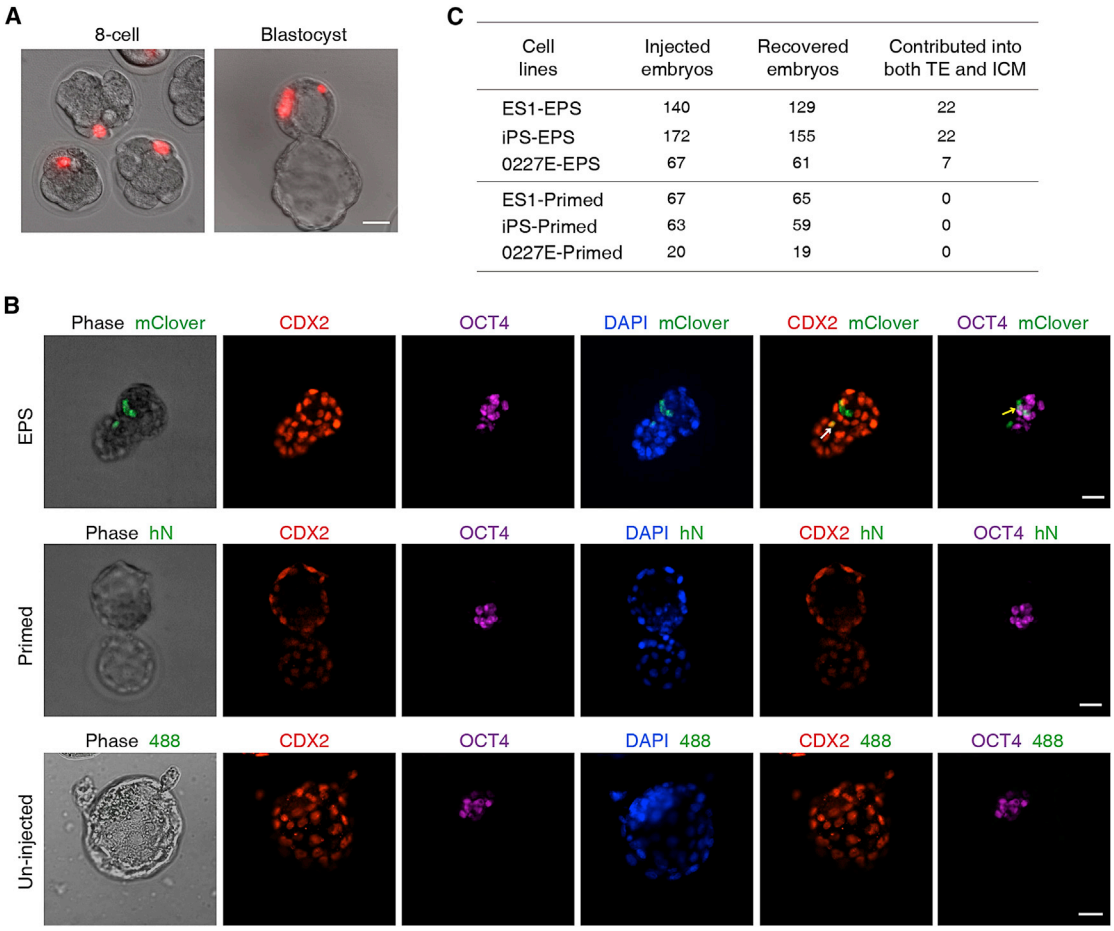

C

Cell lines	Injected embryos	Recovered embryos	Contributed into both TE and ICM
ES1-EPS	140	129	22
iPS-EPS	172	155	22
0227E-EPS	67	61	7
ES1-Primed	67	65	0
iPS-Primed	63	59	0
0227E-Primed	20	19	0

Figure 5. A Single hEPS Cell Can Chimerize Both ICM and TE in Human-Mouse Interspecies Chimeric Blastocysts

(A and B) Diagrams showing a single fluorescent reporter-labeled hEPS cell was microinjected into one mouse 8C embryo, and the injected embryo was cultured for an additional 48–60 hr (A). Then, the embryos were co-immunostained with anti-OCT4 and anti-CDX2 antibodies (B). mClover, direct observation of mClover fluorescent signal; hN, immunostaining of hN; 488, fluorescent signal from the 488 channel. Primed hPSCs were injected as controls. White arrow, mClover$^+$/CDX2$^+$ cells; yellow arrow, mClover$^+$/OCT4$^+$ cells. Scale bars, 20 μm.

(C) Summary of chimeric assays of single-cell injection using hEPS cells at the 8C embryo stage. Contribute into both ICM and TE: embryos with the integration of human cells into both ICM and TE.

See also Figure S5.

clearly detected in the teratomas derived from hEPS cells (Figure S6I). Although these results suggest the possibility that hEPS cells may further differentiate in mouse conceptuses, the limited chimerism of hEPS cells in mouse conceptuses prevented further detailed analysis of the identity of these cells, especially their functionality. Together, albeit limited, these data suggest that hEPS cells do exhibit interspecies chimeric competency in vivo.

Molecular Features of EPS Cells

To characterize the molecular features of EPS cells, we assessed the transcriptomes of mEPS cells, mES cells, two-cell (2C)-like mES-cell subpopulations (Macfarlan et al., 2012), and epiblast stem cells (Najm et al., 2011). Principal component analysis revealed a global gene expression pattern of mEPS cells that was distinct from that of other cell types (Figure 7A). Likewise, hEPS cells also showed distinct transcriptomic features from those of naive hPSCs (Chan et al., 2013; Gafni et al., 2013; Takashima et al., 2014; Theunissen et al., 2014) and primed hPSCs (Figure 7B). We next examined differently expressed genes between mEPS and mES cells (Table S5), and two distinct gene modules (module A and B) stand out among genes upregulated in mEPS cells (Figure 7C and Table S5). Compared to mouse embryonic cells from early preimplantation development (Tang et al., 2011), module A was uniquely presented in mEPS cells, the function of which was involvement in chromatin organization and transcriptional regulation (Table S5). Notably, genes from module B were also expressed in embryonic cells at 2C stage (Figure 7C). Interestingly, the expression levels of genes from module B were gradually downregulated from 2C stage to blastocyst stage. By performing a similar analysis, we identified two gene modules (termed modules C and D) among genes upregulated in hEPS cells, as compared to primed hPSCs (Figure 7D and Table S5). Similarly to module A, genes from module C

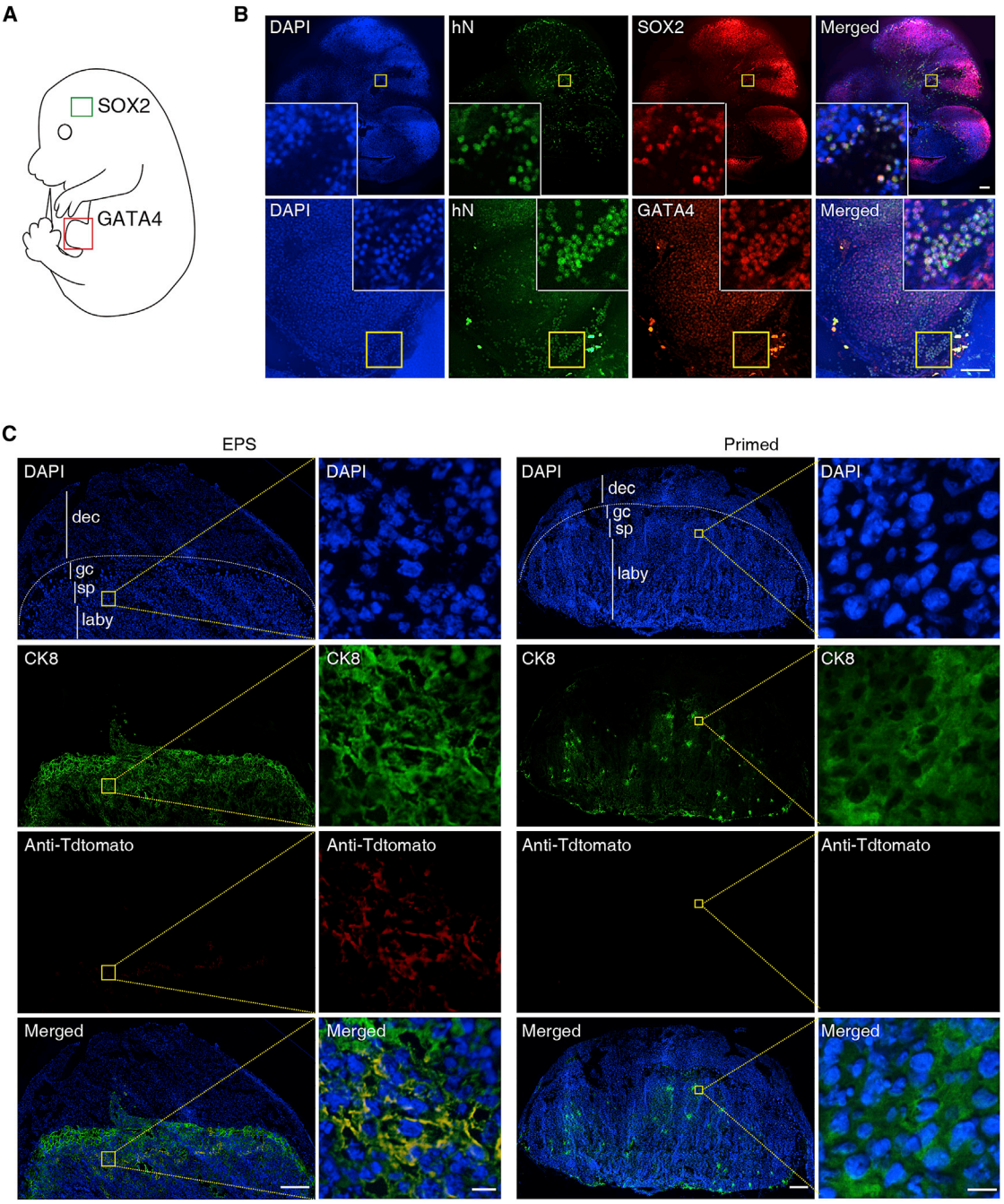

Figure 6. Interspecies Chimerism of hEPS Cells in E10.5 Mouse Conceptuses

(A) Schematic diagram of approximate section planes in hEPS-injected embryos at E10.5. The green and red boxes indicate the sagittal section of brain and heart region respectively.

(B) Representative images showing the integration of hEPS-derived cells into mouse E10.5 embryos. Anti-human nuclei (hN) antibody was co-stained with anti-SOX2 (upper panels, the green box in (A)) and anti-GATA4 (lower panels, the red box in (A)) antibodies. The insets are enlargements of the yellow boxes. The pseudo-colors were used. Scale bars, 100 μm.

(C) Representative whole-placenta confocal images showing Tdtomato-labeled hEPS derivatives can integrate to the trophoblast layers of the E10.5 chimeric placenta by co-staining with anti-Tdtomato and anti-cytokeratin 8 (CK8) antibodies. Primed hPSCs were injected as controls. Scale bars, 200 μm. The right panels are enlargements of the yellow boxes (scale bars, 20 μm). dec, decidua layer; gc, giant cell layer; sp, spongiotrophoblast layer; laby, labyrinth layer. The pseudo-colors were used.

See also Figure S6.

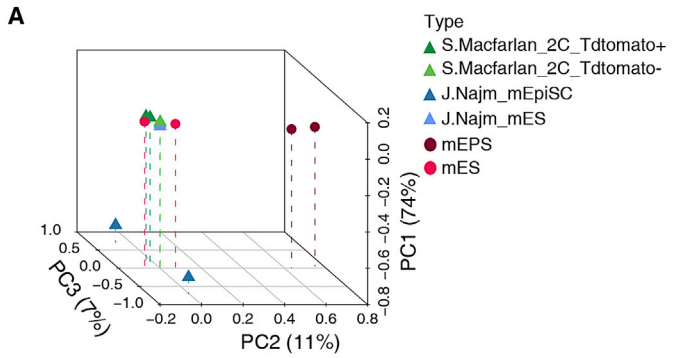

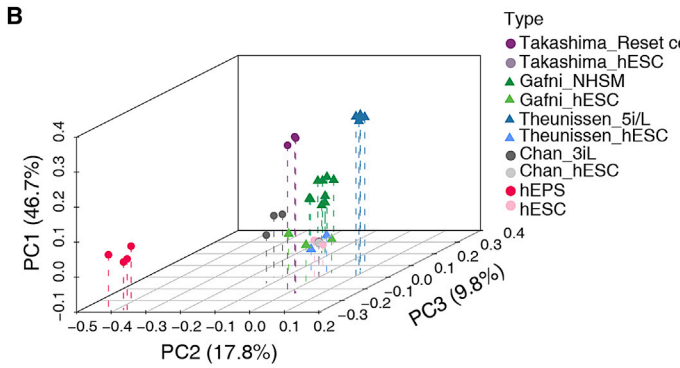

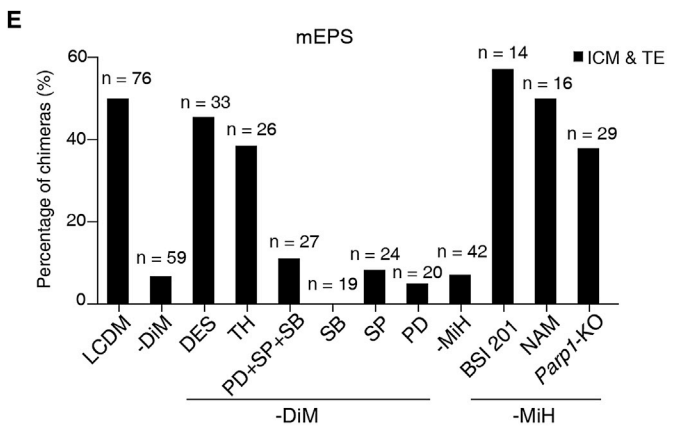

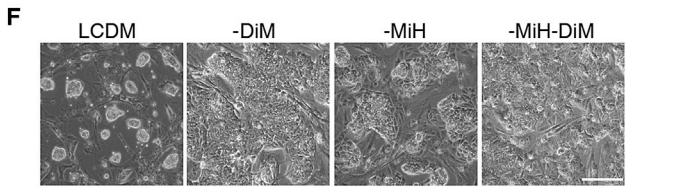

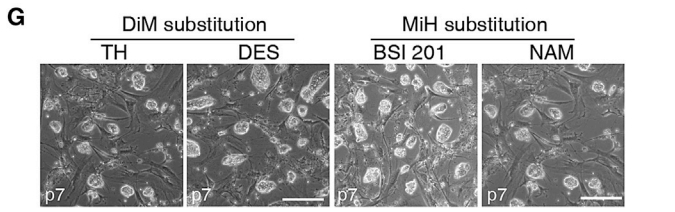

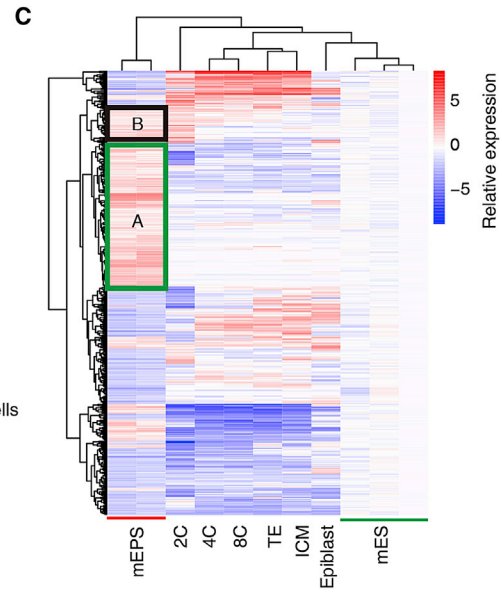

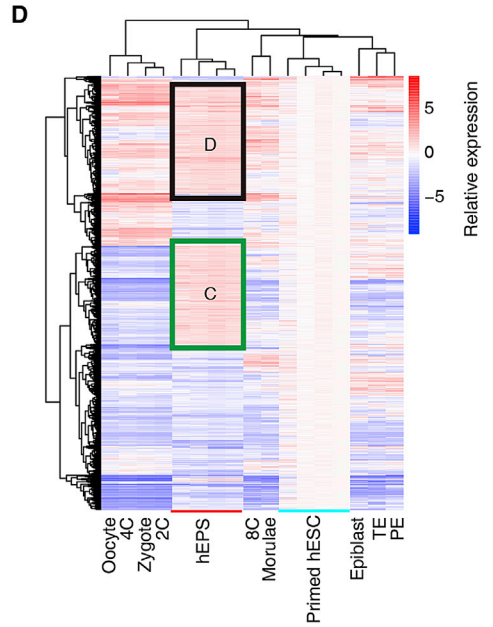

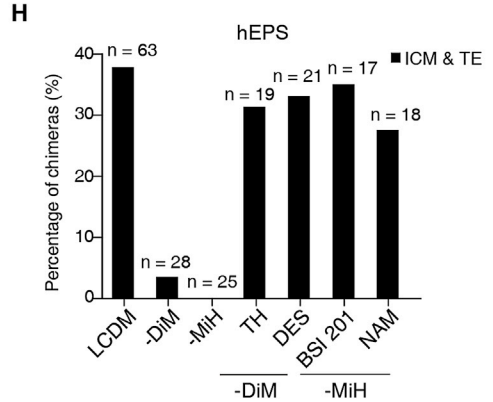

(legend on next page)

were involved in chromatin organization and transcriptional regulation (Table S5), and a significant number of these genes were shared among the naive hPSCs examined (Figure S7A). Notably, a significant number of genes from module D were also found in human embryonic cells from the oocyte to morula stages (Yan et al., 2013) (Figure 7D).

We next examined the epigenetic feature of EPS cells by analyzing the genome-wide distribution of histone 3 lysine 4 trimethylation (H3K4me3) and H3K27me3 chromatin marks in these cells. Compared to naive mES cells, there was no obvious global change of H3K4me3 signals in mEPS cells (Figure S7B). Interestingly, mEPS cells showed a genome-wide increase of H3K27me3 markers (Figure S7B). Furthermore, developmental genes, such as *Tfap2c* and *Cdx2* (Figure S7C), also showed upregulation of H3K27me3 signals in mEPS cells as compared to that in naive mES cells (Figure S7B). We also analyzed the H3K4me3 and H3K27me3 statuses in hEPS cells and primed hPSCs (Figure S7B). Whereas genome-wide H3K4me3 distribution showed no significant difference between these two cell populations, a significant reduction of genome-wide H3K27me3 signals was observed in hEPS cells (Figure S7B). Moreover, developmental genes, such as *HOXA* and *HOXC* clusters (Figure S7D), also showed decreased H3K27me3 distribution in hEPS cells as compared to that in primed hPSCs (Figure S7B). Collectively, these data, combined with the global gene expression profiling, suggest that EPS cells possess unique molecular features distinct from known PSC types.

Mechanistic Exploration of the Roles of DiM and MiH in Maintaining EPS Cells

Finally, we investigated the roles of DiM and MiH in maintaining EPS cells. The withdrawal of either DiM or MiH significantly impaired the developmental potency of mEPS cells in chimeric blastocysts (Figure 7E and Table S6) and led to rapid differentiation of primed hPSC-converted hEPS cells (Figure 7F). DiM has been reported to inhibit G protein coupled receptors, including the histamine and the muscarinic receptors (Pfaff et al., 1995), and MiH is known to inhibit PARP1 (Alano et al., 2006). Notably, DiM or MiH could be replaced with other inhibitors targeting the same targets for the maintenance of hEPS cells (Figure 7G). Importantly, both mEPS and hEPS cells still retained their ability to contribute to both TE and ICM in blastocysts under such conditions (Figures 7E and 7H and Table S6).

We next attempted to explore the molecular targets regulated by DiM and MiH in EPS cells. MAPK signaling has been reported to be the major downstream signaling of histamine and muscarinic receptor signaling (Ockenga et al., 2013). Similarly to naive mES cells, MAPK signaling activities were downregulated in mEPS cells (Figure S7E). Compared to primed hPSCs, the downregulation of MAPK signaling activities was observed in hEPS cells (Figure S7F). However, replacement of DiM with inhibitors targeting to MAPK signaling could not maintain hEPS cells (Figure S7G) and could not preserve the developmental potency of mEPS cells (Figure 7E and Table S6). To further examine the role of MiH, we knocked out *Parp1*, a proposed molecular target of MiH, in mEPS cell lines (Figures S7H–S7L). Importantly, *Parp1*-deficient mEPS cells could still contribute to both TE and ICM even in the absence of MiH (Figure 7E and Table S6). These results suggest that *Parp1* is an important regulator in the maintenance of EPS cell developmental potency.

DISCUSSION

In this study, we identify a specific chemical cocktail that enables the generation and long-term propagation of EPS cell lines with both Em and ExEm differentiation potentials. The developmental potency of EPS cells was demonstrated at the single-cell level. EPS cells possess unique transcriptomic features distinct from known PSCs. Mechanistic analyses suggest that chemical inhibitions of *PARP1* and histamine and muscarinic receptor signaling are critical for the maintenance of EPS cells' developmental potential.

One notable functional feature of mEPS cells is their robust ability to generate single-cell-derived chimeras. Generating chimeras by using single cells is considered a highly stringent assay for evaluating the developmental potency of PSCs (De Los Angeles et al., 2015). Notably, single mEPS cells showed robust chimeric contribution to conceptuses from middle to

Figure 7. Analyses of Molecular Features of EPS Cells and the Roles of DiM and MiH in Maintaining EPS Developmental Potency

(A and B) PCA analysis of RNA-seq and microarray data from EPS cells and known PSC types. Log2 expression values were normalized to mES cells (A) or primed hPSCs (B) in each study. For (A), data from mEPS cells (this study), mES cells (each study), 2C-like cells (Macfarlan et al. (2012)), and epiblast stem cells (Najm et al. (2011)) were analyzed, and a total of 17,243 genes were selected. For (B), data from hEPS cells (this study), naive hPSCs (Takashima et al. (2014), Chan et al. (2013), Gafni et al. (2013), and Theunissen et al. (2014)), and primed hPSCs (each study) were analyzed, and a total of 15,958 genes were selected. Circles, RNA-seq data; triangles, microarray data.

(C and D) Heatmaps showing the presence of EPS-specific gene modules in mEPS (C) and hEPS (D) cells when compared to mES cells (C) and primed hPSCs (D) respectively. Correlations between genes and samples were calculated using Euclidean distance (complete linkage). Log2 expression values were normalized to mES cells (C) or primed hPSCs (D) in each study. hESC, primed hPSCs. To compare EPS cells with embryonic cells from preimplantation stages, data from Tang et al. (2011) (C) and Yan et al. (2013) (D) were analyzed.

(E) Analyses of the influence of DiM or MiH substitution and *Parp1* knockout on the chimeric ability of mEPS cells. Multiple cells were injected. The bar chart shows the percentage of chimeras among the recovered blastocysts. n indicates numbers of recovered blastocysts. ICM & TE, embryos with the integration of mouse cells into both ICM and TE.

(F) Representative images of hEPS colonies after the omission of DiM, MiH or both from the LCDM condition. Scale bar, 100 μm.

(G) Representative images of hEPS colonies at passage 7 after DiM or MiH substitution. Scale bars, 100 μm.

(H) Analyses of the influence of DiM or MiH substitution on the chimeric ability of hEPS cells. Multiple cells were injected. The bar chart shows the percentage of chimeras among the recovered blastocysts. n indicates numbers of recovered blastocysts. ICM & TE, embryos with the integration of human cells into both ICM and TE.

TH, tripelennamine HCL; DES, desloratadine; NAM, nicotinamide. PD, PD 0325901; SB, SB 203580; SP: SP 600125.

See also Figure S7.

late gestation stages (Table S3), accompanied by widespread integration in both embryonic and ExEm parts (Figures 4A and S4A). Furthermore, we also obtained single-mEPS-cell-derived adult germline competent chimeras (Figures 4F and 4G and Table S3). Remarkably, single mEPS cells could produce entire mice by tetraploid complementation (Figures 4H and S4H and S4I). Interestingly, we observed that the efficiency of single-cell chimerism for mEPS cells (60.1%) was higher than that of mouse ES cells (20.8%) at the blastocyst stage (Table S3).

Another notable finding is that human EPS cells show robust interspecies chimerism in mouse conceptus (Figure 5 and 6 and S5 and S6). Although primed hPSCs could chimerize mouse embryos at the post-implantation stage (Mascetti and Pedersen, 2016b; Wu et al., 2015), generation of interspecies chimeras by injecting hPSCs into preimplantation mouse blastocysts proves to be extremely challenging (Mascetti and Pedersen, 2016a; Wu et al., 2016). Compared to a previous report (Theunissen et al., 2016), the percentage of mouse embryos retaining human EPS cells (34.4%) is significantly higher than that with naive hPSCs (0.88%, 7/799 dissected embryos). Furthermore, the level of chimeric integration of hEPS cells could be up to 1%, which is also higher than naive hPSCs (0.05%) (Theunissen et al., 2016). More importantly, immunostaining and RT-PCR analyses of the fate of chimeric human EPS derivatives further implies that human EPS cells may further differentiate in mouse conceptuses (Figure 6 and S6G and S6H). The enhanced interspecies chimerism of human EPS cells may be explained by their increased proliferative rate and improved single-cell survival (Figures S1B and S1C). In support of this notion, overexpression of the anti-apoptotic factor BCL2 confers rat epiblast stem cells interspecies chimerism in mouse embryos (Masaki et al., 2016). It should be noted, however, that the interspecies chimerism of human EPS cells in mouse conceptuses is still limited. To further enhance the level of human EPS cell contribution, strategies including interspecies blastocyst complementation and choosing an evolutionarily and/or developmentally closer host may help (Wu et al., 2016; Wu et al., 2017).

Intriguingly, human EPS cells also integrate into ExEm tissues in interspecies chimeric mouse conceptuses. Single-hEPS-cell derivations can integrate into the TE layer of mouse blastocysts and express TE markers (Figures 5B and S5), suggesting that they may have adopted the TE fate. Upon further in vivo development, differentiated hEPS cells expressing the trophoblast marker CK8 were observed in the trophoblast layers in E10.5 human-mouse chimeric placentas (Figure 6C). Of note, the presence of human cells was not detected in the control primed hPSC group (Figure 6C). These findings are unexpected, since human and mouse placentas are structurally different due to heterochronic and/or divergent placental developmental programs (Rossant and Cross, 2001). Indeed, despite the presence of human cells, the level of human EPS cells' contribution in the mouse placenta is very limited.

The unique bi-directional developmental potency of EPS cells raises an important question of whether they resemble embryonic cells from early preimplantation stages. It has been reported that a rare transient population with 2C-like features exist in mES cell cultures (Macfarlan et al., 2012). Interestingly, the 2C-like molecular features were not observed in mEPS cells. Regardless, Gene Ontology terms of gene modules overrepresented in hEPS cells were similar to those found specifically marking zygotes to the four-cell (4C) stage (Xue et al., 2013) (Figure 7D and Table S5), suggesting some molecular features from early pre-implantation are retained in EPS cells. On the other hand, it should be noted that the global gene expression pattern of EPS cells is distinct from that of embryonic cells from 2C to 4C stages (data not shown). Similarly, at the whole transcriptomic level, 2C-like cells were distinct from 2C embryos (Kolodziejczyk et al., 2015). This is not surprising considering the complexity of the in vivo niche and developmental processes, e.g., asymmetric epigenetic regulation of paternal and maternal genomes (Cantone and Fisher, 2013). The absence of these parameters in cultured cell lines might have contributed to the observed differences. Alternatively, it is also possible that EPS cells may reside in a state that is somewhat different from in vivo development, which needs to be explored in future studies.

Finally, our findings reveal an important role of PARP1 inhibition in maintaining EPS potency. PARP1 is a nuclear protein responsible for poly-ADP-ribosylation, which has also been shown to regulate transcription and chromatin remodeling (Hassa and Hottiger, 2008). In our study, PARP1 inhibition did not impair the self-renewal of EPS cells but was found to be required for the maintenance of their developmental potency (Figure 7E). Notably, *Parp1* deficiency in mouse ES cells induced their differentiation into trophoblast derivatives (Hemberger et al., 2003; Nozaki et al., 2013), and upregulation of ExEm differentiation pathways was observed in *Parp1*$^{-/-}$ mouse ES cells (Ogino et al., 2007). Consistent with these observations, our results further suggest that *Parp1* might be involved in the regulation of ExEm developmental potency. Interestingly, *PARP1* expression gradually increases from 8C to blastocyst stage in human preimplantation development (Yan et al., 2013). These reports, together with our findings, raise the important question of whether *Parp1* participates in lineage determination during preimplantation development.

Overall, our study demonstrates the feasibility of generating stable stem cell lines with both Em and ExEm developmental potency. EPS cell lines provide a useful cellular tool for gaining a better molecular understanding of initial cell fate commitments and generating new animal models to investigate basic questions concerning development of the placenta, yolk sac, and embryo proper (Leung and Zernicka-Goetz, 2015; Wu and Izpisua Belmonte, 2016). Furthermore, they also provide an unlimited cell resource and hold great potential for in vivo disease modeling, in vivo drug discovery, and in vivo tissue generation in the future. Finally, our study opens a path toward capturing stem cells with intra- and/or inter-species bi-potent chimeric competency from a variety of other mammalian species.

STAR★METHODS

Detailed methods are provided in the online version of this paper and include the following:

- KEY RESOURCES TABLE
- CONTACT FOR REAGENT AND RESOURCE SHARING
- EXPERIMENTAL MODEL AND SUBJECT DETAILS

SUPPLEMENTAL INFORMATION

Supplemental Information includes seven figures and seven tables.

A video abstract is available at http://dx.doi.org/10.1016/j.cell.2017.02.005#mmc8.

AUTHOR CONTRIBUTIONS

Y.Y., B.L., J.X., J.L.W., and H.K.D. designed the study and performed and interpreted experiments. Some experiments were designed and/or performed as the result of the collaboration between the H.K.D. and the J.C.I.B. groups. J.W. helped with human EPS cell culture and chimeric experiments. Y.X.X. and J.B.D helped with the experiments. C.S. and H.S offered technical support in assay of human EPS derivation from human blastocysts. F.Y.S., X.Y.L., Y.Q.D., T.W., C.R.Z., H.B.L., S.G.D., M.Y., and W.F.Y conducted microinjections and mouse breeding. C.Y.W., W.F.L., X.L., and D.C.Z. assisted in differentiation of EPS in vivo and in vitro. C.L. and A.B.H. helped with ChIP-seq analysis. Y.F.L. and C.L. helped with RNA-seq analysis. H.X.L. assisted in embryo imaging. J.L.Z. and X.L conducted in gene expression analysis of cells. X.C.C and H.Z. performed immunostaining of teratomas. J.W., T.Y., A.S., Z.L., and J.C.I.B independently repeated the main results. H.K.D. conceived and supervised this project and wrote the paper with Y.Y., B.L., J.X., J.W., and J.C.I.B.

ACKNOWLEDGMENTS

We thank L.Y. Du, X. Ch. Li, C.Y. Shan, Y. Xie, Q. Huo, Y. Tian, C. Han, S.W. Duan, L.J. Cheng, and K. Zhang for technical assistance and thank the Core Facilities at School of Life Sciences, Peking University for technical assistance, especially Lu H. X. We thank X. Zhang, Y.Q. Li, J.Y. Guan, T. Zhao, K. Liu, Y.Y. Du, and R.G. Fang for discussions in the course of the preparation of this manuscript. This work was supported by the National Key Research and Development Program of China (2016YFA0100100), the National Natural Science Foundation of China (31521004), the Guangdong Innovative and Entrepreneurial Research Team Program (2014ZT05S216), the Science and Technology Planning Project of Guangdong Province, China (2014B020226001), the Science and Technology Program of Guangzhou, China (2016B030232001), and the Ministry of Education of China (111 Project). This work was supported in part by a grant from the BeiHao Stem Cell and Regenerative Medicine Translational Research Institute and a collaborative pilot grant by the Joint Institute of Peking University Health Science Center and University of Michigan Health System. J.X. was supported in part by the Postdoctoral Fellowship of Peking-Tsinghua Center for Life Sciences. C.Y.W. was supported by the National Science and Technology Support Project (2014BAI02B01). S.G.D. was supported by the CAS Key Technology Talent Program. Work in the laboratory of J.C.I.B. was supported by the G. Harold and Leila Y. Mathers Charitable Foundation and The Moxie Foundation.

Received: December 20, 2016
Revised: January 24, 2017
Accepted: February 1, 2017
Published: April 6, 2017

REFERENCES

Abad, M., Mosteiro, L., Pantoja, C., Cañamero, M., Rayon, T., Ors, I., Graña, O., Megías, D., Domínguez, O., Martínez, D., et al. (2013). Reprogramming in vivo produces teratomas and iPS cells with totipotency features. Nature *502*, 340–345.

Alano, C.C., Kauppinen, T.M., Valls, A.V., and Swanson, R.A. (2006). Minocycline inhibits poly(ADP-ribose) polymerase-1 at nanomolar concentrations. Proc. Natl. Acad. Sci. USA *103*, 9685–9690.

Beddington, R.S., and Robertson, E.J. (1989). An assessment of the developmental potential of embryonic stem cells in the midgestation mouse embryo. Development *105*, 733–737.

Brons, I.G., Smithers, L.E., Trotter, M.W., Rugg-Gunn, P., Sun, B., Chuva de Sousa Lopes, S.M., Howlett, S.K., Clarkson, A., Ahrlund-Richter, L., Pedersen, R.A., and Vallier, L. (2007). Derivation of pluripotent epiblast stem cells from mammalian embryos. Nature *448*, 191–195.

Buehr, M., Meek, S., Blair, K., Yang, J., Ure, J., Silva, J., McLay, R., Hall, J., Ying, Q.L., and Smith, A. (2008). Capture of authentic embryonic stem cells from rat blastocysts. Cell *135*, 1287–1298.

Cantone, I., and Fisher, A.G. (2013). Epigenetic programming and reprogramming during development. Nat. Struct. Mol. Biol. *20*, 282–289.

Chan, Y.S., Göke, J., Ng, J.H., Lu, X., Gonzales, K.A.U., Tan, C.P., Tng, W.Q., Hong, Z.Z., Lim, Y.S., and Ng, H.H. (2013). Induction of a human pluripotent state with distinct regulatory circuitry that resembles preimplantation epiblast. Cell Stem Cell *13*, 663–675.

Chen, Y., Niu, Y., Li, Y., Ai, Z., Kang, Y., Shi, H., Xiang, Z., Yang, Z., Tan, T., Si, W., et al. (2015). Generation of Cynomolgus Monkey Chimeric Fetuses using Embryonic Stem Cells. Cell Stem Cell *17*, 116–124.

Cohen, M.A., Wert, K.J., Goldmann, J., Markoulaki, S., Buganim, Y., Fu, D., and Jaenisch, R. (2016). Human neural crest cells contribute to coat pigmentation in interspecies chimeras after in utero injection into mouse embryos. Proc. Natl. Acad. Sci. USA *113*, 1570–1575.

De Los Angeles, A., Ferrari, F., Xi, R., Fujiwara, Y., Benvenisty, N., Deng, H., Hochedlinger, K., Jaenisch, R., Lee, S., Leitch, H.G., et al. (2015). Hallmarks of pluripotency. Nature *525*, 469–478.

Evans, M.J., and Kaufman, M.H. (1981). Establishment in culture of pluripotential cells from mouse embryos. Nature *292*, 154–156.

Fang, R., Liu, K., Zhao, Y., Li, H., Zhu, D., Du, Y., Xiang, C., Li, X., Liu, H., Miao, Z., et al. (2014). Generation of naive induced pluripotent stem cells from rhesus monkey fibroblasts. Cell Stem Cell *15*, 488–496.

Gafni, O., Weinberger, L., Mansour, A.A., Manor, Y.S., Chomsky, E., Ben-Yosef, D., Kalma, Y., Viukov, S., Maza, I., Zviran, A., et al. (2013). Derivation of novel human ground state naive pluripotent stem cells. Nature *504*, 282–286.

Guo, G., von Meyenn, F., Santos, F., Chen, Y., Reik, W., Bertone, P., Smith, A., and Nichols, J. (2016). Naive Pluripotent Stem Cells Derived Directly from Isolated Cells of the Human Inner Cell Mass. Stem Cell Reports *6*, 437–446.

Hassa, P.O., and Hottiger, M.O. (2008). The diverse biological roles of mammalian PARPS, a small but powerful family of poly-ADP-ribose polymerases. Front. Biosci. *13*, 3046–3082.

Hemberger, M., Nozaki, T., Winterhager, E., Yamamoto, H., Nakagama, H., Kamada, N., Suzuki, H., Ohta, T., Ohki, M., Masutani, M., and Cross, J.C. (2003). Parp1-deficiency induces differentiation of ES cells into trophoblast derivatives. Dev. Biol. *257*, 371–381.

Huang, D.W., Sherman, B.T., and Lempicki, R.A. (2009a). Bioinformatics enrichment tools: paths toward the comprehensive functional analysis of large gene lists. Nucleic acids research *37*, 1–13.

Huang, D.W., Sherman, B.T., and Lempicki, R.A. (2009b). Systematic and integrative analysis of large gene lists using DAVID bioinformatics resources. Nature protocols *4*, 44–57.

James, D., Noggle, S.A., Swigut, T., and Brivanlou, A.H. (2006). Contribution of human embryonic stem cells to mouse blastocysts. Dev. Biol. *295*, 90–102.

Kolodziejczyk, A.A., Kim, J.K., Tsang, J.C., Ilicic, T., Henriksson, J., Natarajan, K.N., Tuck, A.C., Gao, X., Bühler, M., Liu, P., et al. (2015). Single Cell RNA-Sequencing of Pluripotent States Unlocks Modular Transcriptional Variation. Cell Stem Cell *17*, 471–485.

Kunath, T., Arnaud, D., Uy, G.D., Okamoto, I., Chureau, C., Yamanaka, Y., Heard, E., Gardner, R.L., Avner, P., and Rossant, J. (2005). Imprinted X-inactivation in extra-embryonic endoderm cell lines from mouse blastocysts. Development *132*, 1649–1661.

Lerdrup, M., Johansen, J.V., Agrawal-Singh, S., and Hansen, K. (2016). An interactive environment for agile analysis and visualization of ChIP-sequencing data. Nature structural & molecular biology *23*, 349–357.

Leung, C.Y., and Zernicka-Goetz, M. (2015). Mapping the journey from totipotency to lineage specification in the mouse embryo. Curr. Opin. Genet. Dev. *34*, 71–76.

Li, H., and Durbin, R. (2009). Fast and accurate short read alignment with Burrows-Wheeler transform. Bioinformatics *25*, 1754–1760.

Li, P., Tong, C., Mehrian-Shai, R., Jia, L., Wu, N., Yan, Y., Maxson, R.E., Schulze, E.N., Song, H., Hsieh, C.L., et al. (2008). Germline competent embryonic stem cells derived from rat blastocysts. Cell *135*, 1299–1310.

Love, M.I., Huber, W., and Anders, S. (2014). Moderated estimation of fold change and dispersion for RNA-seq data with DESeq2. Genome biology *15*, 550.

Macfarlan, T.S., Gifford, W.D., Driscoll, S., Lettieri, K., Rowe, H.M., Bonanomi, D., Firth, A., Singer, O., Trono, D., and Pfaff, S.L. (2012). Embryonic stem cell potency fluctuates with endogenous retrovirus activity. Nature *487*, 57–63.

Martin, G.R. (1981). Isolation of a pluripotent cell line from early mouse embryos cultured in medium conditioned by teratocarcinoma stem cells. Proc. Natl. Acad. Sci. USA *78*, 7634–7638.

Masaki, H., Kato-Itoh, M., Takahashi, Y., Umino, A., Sato, H., Ito, K., Yanagida, A., Nishimura, T., Yamaguchi, T., Hirabayashi, M., et al. (2016). Inhibition of Apoptosis Overcomes Stage-Related Compatibility Barriers to Chimera Formation in Mouse Embryos. Cell Stem Cell *19*, 587–592.

Mascetti, V.L., and Pedersen, R.A. (2016a). Contributions of Mammalian Chimeras to Pluripotent Stem Cell Research. Cell Stem Cell *19*, 163–175.

Mascetti, V.L., and Pedersen, R.A. (2016b). Human-Mouse Chimerism Validates Human Stem Cell Pluripotency. Cell Stem Cell *18*, 67–72.

Morgani, S.M., Canham, M.A., Nichols, J., Sharov, A.A., Migueles, R.P., Ko, M.S., and Brickman, J.M. (2013). Totipotent embryonic stem cells arise in ground-state culture conditions. Cell Rep. *3*, 1945–1957.

Najm, F.J., Chenoweth, J.G., Anderson, P.D., Nadeau, J.H., Redline, R.W., McKay, R.D., and Tesar, P.J. (2011). Isolation of epiblast stem cells from preimplantation mouse embryos. Cell Stem Cell *8*, 318–325.

Nichols, J., and Smith, A. (2009). Naive and primed pluripotent states. Cell Stem Cell *4*, 487–492.

Nozaki, T., Fujimori, H., Wang, J., Suzuki, H., Imai, H., Watanabe, M., Ohura, K., and Masutani, M. (2013). Parp-1 deficiency in ES cells promotes invasive and metastatic lesions accompanying induction of trophoblast giant cells during tumorigenesis in uterine environment. Pathol. Int. *63*, 408–414.

Ockenga, W., Kühne, S., Bocksberger, S., Banning, A., and Tikkanen, R. (2013). Non-neuronal functions of the m2 muscarinic acetylcholine receptor. Genes (Basel) *4*, 171–197.

Ogino, H., Nozaki, T., Gunji, A., Maeda, M., Suzuki, H., Ohta, T., Murakami, Y., Nakagama, H., Sugimura, T., and Masutani, M. (2007). Loss of Parp-1 affects gene expression profile in a genome-wide manner in ES cells and liver cells. BMC Genomics *8*, 41.

Papaioannou, V.E., Mkandawire, J., and Biggers, J.D. (1989). Development and phenotypic variability of genetically identical half mouse embryos. Development *106*, 817–827.

Pfaff, O., Hildebrandt, C., Waelbroeck, M., Hou, X., Moser, U., Mutschler, E., and Lambrecht, G. (1995). The (S)-(+)-enantiomer of dimethindene: a novel M2-selective muscarinic receptor antagonist. Eur. J. Pharmacol. *286*, 229–240.

Rossant, J., and Cross, J.C. (2001). Placental development: lessons from mouse mutants. Nat. Rev. Genet. *2*, 538–548.

Rossant, J., and Tam, P.P. (2017). New Insights into Early Human Development: Lessons for Stem Cell Derivation and Differentiation. Cell Stem Cell *20*, 18–28.

Shen, L., Shao, N., Liu, X., and Nestler, E. (2014). ngs. plot: Quick mining and visualization of next-generation sequencing data by integrating genomic databases. BMC genomics *15*, 284.

Tachibana, M., Sparman, M., Ramsey, C., Ma, H., Lee, H.S., Penedo, M.C., and Mitalipov, S. (2012). Generation of chimeric rhesus monkeys. Cell *148*, 285–295.

Takashima, Y., Guo, G., Loos, R., Nichols, J., Ficz, G., Krueger, F., Oxley, D., Santos, F., Clarke, J., Mansfield, W., et al. (2014). Resetting transcription factor control circuitry toward ground-state pluripotency in human. Cell *158*, 1254–1269.

Tanaka, S., Kunath, T., Hadjantonakis, A.K., Nagy, A., and Rossant, J. (1998). Promotion of trophoblast stem cell proliferation by FGF4. Science *282*, 2072–2075.

Tang, F., Barbacioru, C., Nordman, E., Bao, S., Lee, C., Wang, X., Tuch, B.B., Heard, E., Lao, K., and Surani, M.A. (2011). Deterministic and stochastic allele specific gene expression in single mouse blastomeres. PLoS ONE *6*, e21208.

Tarkowski, A.K. (1959). Experiments on the development of isolated blastomers of mouse eggs. Nature *184*, 1286–1287.

Tesar, P.J., Chenoweth, J.G., Brook, F.A., Davies, T.J., Evans, E.P., Mack, D.L., Gardner, R.L., and McKay, R.D. (2007). New cell lines from mouse

epiblast share defining features with human embryonic stem cells. Nature *448*, 196–199.

Theunissen, T.W., Powell, B.E., Wang, H., Mitalipova, M., Faddah, D.A., Reddy, J., Fan, Z.P., Maetzel, D., Ganz, K., Shi, L., et al. (2014). Systematic identification of culture conditions for induction and maintenance of naive human pluripotency. Cell Stem Cell *15*, 471–487.

Theunissen, T.W., Friedli, M., He, Y., Planet, E., O'Neil, R.C., Markoulaki, S., Pontis, J., Wang, H., Iouranova, A., Imbeault, M., et al. (2016). Molecular Criteria for Defining the Naive Human Pluripotent State. Cell Stem Cell *19*, 502–515.

Thomson, J.A., Itskovitz-Eldor, J., Shapiro, S.S., Waknitz, M.A., Swiergiel, J.J., Marshall, V.S., and Jones, J.M. (1998). Embryonic stem cell lines derived from human blastocysts. Science *282*, 1145–1147.

Trapnell, C., Pachter, L., and Salzberg, S.L. (2009). TopHat: discovering splice junctions with RNA-Seq. Bioinformatics *25*, 1105–1111.

Vallier, L., Alexander, M., and Pedersen, R.A. (2005). Activin/Nodal and FGF pathways cooperate to maintain pluripotency of human embryonic stem cells. J. Cell Sci. *118*, 4495–4509.

Wang, J., Xie, G., Singh, M., Ghanbarian, A.T., Raskó, T., Szvetnik, A., Cai, H., Besser, D., Prigione, A., Fuchs, N.V., et al. (2014). Primate-specific endogenous retrovirus-driven transcription defines naive-like stem cells. Nature *516*, 405–409.

Ware, C.B., Nelson, A.M., Mecham, B., Hesson, J., Zhou, W., Jonlin, E.C., Jimenez-Caliani, A.J., Deng, X., Cavanaugh, C., Cook, S., et al. (2014). Derivation of naive human embryonic stem cells. Proc. Natl. Acad. Sci. USA *111*, 4484–4489.

Wu, J., and Izpisua Belmonte, J.C. (2016). The Molecular Harbingers of Early Mammalian Embryo Patterning. Cell *165*, 13–15.

Wu, J., Okamura, D., Li, M., Suzuki, K., Luo, C., Ma, L., He, Y., Li, Z., Benner, C., Tamura, I., et al. (2015). An alternative pluripotent state confers interspecies chimaeric competency. Nature *521*, 316–321.

Wu, J., Greely, H.T., Jaenisch, R., Nakauchi, H., Rossant, J., and Belmonte, J.C. (2016). Stem cells and interspecies chimaeras. Nature *540*, 51–59.

Wu, J., Platero-Luengo, A., Sakurai, M., Sugawara, A., Gil, M.A., Yamauchi, T., Suzuki, K., Bogliotti, Y.S., Cuello, C., Morales Valencia, M., et al. (2017). Interspecies chimerism with mammalian pluripotent stem cells. Cell *168*, 473–486.e15.

Xue, Z., Huang, K., Cai, C., Cai, L., Jiang, C.Y., Feng, Y., Liu, Z., Zeng, Q., Cheng, L., Sun, Y.E., et al. (2013). Genetic programs in human and mouse early embryos revealed by single-cell RNA sequencing. Nature *500*, 593–597.

Yan, L., Yang, M., Guo, H., Yang, L., Wu, J., Li, R., Liu, P., Lian, Y., Zheng, X., Yan, J., et al. (2013). Single-cell RNA-Seq profiling of human preimplantation embryos and embryonic stem cells. Nat. Struct. Mol. Biol. *20*, 1131–1139.

Yeom, Y.I., Fuhrmann, G., Ovitt, C.E., Brehm, A., Ohbo, K., Gross, M., Hübner, K., and Schöler, H.R. (1996). Germline regulatory element of Oct-4 specific for the totipotent cycle of embryonal cells. Development *122*, 881–894.

Ying, Q.L., Wray, J., Nichols, J., Batlle-Morera, L., Doble, B., Woodgett, J., Cohen, P., and Smith, A. (2008). The ground state of embryonic stem cell self-renewal. Nature *453*, 519–523.

Zhang, Y., Liu, T., Meyer, C.A., Eeckhoute, J., Johnson, D.S., Bernstein, B.E., Nusbaum, C., Myers, R.M., Brown, M., and Li, W. (2008). Model-based analysis of ChIP-Seq (MACS). Genome biology *9*, R137.

STAR★METHODS

KEY RESOURCES TABLE

REAGENT or RESOURCE	SOURCE	IDENTIFIER
Antibodies		
Anti-Cytokeratin 8 (M20)	Santa Cruz Biotechnology	Cat# sc-52324; RRID:AB_629847
Anti-Proliferin (C-14)	Santa Cruz Biotechnology	Cat# sc-47345; RRID:AB_785326
Anti-GATA4 (C-20)	Santa Cruz Biotechnology	Cat# sc-1237; RRID:AB_2108747
Anti-Sox-2 (Y-17)	Santa Cruz Biotechnology	Cat# sc-17320; RRID:AB_2286684
Anti-Oct-3/4 (C-10)	Santa Cruz Biotechnology	Cat# sc-5279; RRID:AB_628051
Anti-GKLF (H-180)	Santa Cruz Biotechnology	Cat# sc-20691; RRID:AB_669567
Anti-LHX5 (KP-02)	Santa Cruz Biotechnology	Cat# sc-130469; RRID:AB_2135825
Anti-beta3 Tubulin (AA10)	Santa Cruz Biotechnology	Cat# sc-80016; RRID:AB_2210523
Anti-PARP-1/2 (H-250)	Santa Cruz Biotechnology	Cat# sc-7150; RRID:AB_2160738
Anti-GATA3 (HG3-31)	Santa Cruz Biotechnology	Cat# sc-268; RRID: AB_2108591
Anti-Trophoblast specific protein alpha	Abcam	Cat# ab104401; RRID:AB_10901888
Anti-Nanog	Abcam	Cat# ab80892; RRID:AB_2150114
Anti-FOXA2	Abcam	Cat# ab60721; RRID:AB_941632
Anti-Mouse TBR2/Eomes	Abcam	Cat# ab23345; RRID:AB_778267
Anti-Oct4	Abcam	Cat# ab18976; RRID:AB_444714
Anti-Sall4	Abcam	Cat# ab29112; RRID:AB_777810
Anti-Oct4 [EPR17929]-ChIP Grade	Abcam	Cat# ab181557
Anti-hCG beta [EPHCGR2]	Abcam	Cat# ab131170; RRID:AB_11156864
Anti-Nuclei, clone 235-1	Millipore	Cat# MAB1281; RRID:AB_94090
Anti-trimethyl-Histone H3 (Lys27)	Millipore	Cat# 07-449; RRID:AB_310624
Anti-Actin, smooth muscle, clone ASM-1	Millipore	Cat# CBL171; RRID:AB_2223166
Anti-trimethyl-Histone H3 (Lys4)	Millipore	Cat# 07-473; RRID:AB_1977252
Anti-p38 MAPK	Cell Signaling Technology	Cat# 9212 also 9212S, 9212L, 9212P; RRID:AB_330713
Anti-Phospho-p38 MAPK (Thr180/Tyr182) (3D7)	Cell Signaling Technology	Cat# 9215 also 9215S, 9215L; RRID:AB_331762
Anti-rabbit IgG, HRP-linked	Cell Signaling Technology	Cat# 7074; RRID:AB_2099233
Anti-mouse IgG, HRP-linked	Cell Signaling Technology	Cat# 7076 also 7076S, 7076V, 7076P2; RRID:AB_330924
Anti-beta-Actin, Clone AC-15	Sigma-Aldrich	Cat# A1978; RRID:AB_476692
Anti-KRT8	Sigma-Aldrich	Cat# HPA049866
Anti-CDX-2, Clone CDX2-88	BioGenex	Cat# AM392
Anti-Cytokeratin 7 (OV-TL 12/30)	Thermo Fisher Scientific	Cat# MA5-11986; RRID:AB_10989596
Anti-tdTomato	Biorbyt	Cat# orb182397
Anti-p44/42 MAPK	Beyotime Technology	Cat# AM076
Anti-Phospho-p44/42 MAPK	Beyotime Technology	Cat# AM071
Anti-JNK/SAPK	Beyotime Technology	Cat# AJ518
HRP conjugated Anti-Rabbit IgG	ZSGB-BIO	ZDR-5306
Alexa Fluor 488-AffiniPure Donkey Anti-Mouse IgG (H+L)	Jackson ImmunoResearch	Cat# 715-545-150; RRID:AB_2340846
Alexa Fluor 488-AffiniPure Donkey Anti-Rabbit IgG (H+L)	Jackson ImmunoResearch	Cat# 711-545-152; RRID:AB_2313584
Alexa Fluor 488-AffiniPure Donkey Anti-Goat IgG (H+L)	Jackson ImmunoResearch	Cat# 705-545-147; RRID:AB_2336933

(*Continued on next page*)

Continued

REAGENT or RESOURCE	SOURCE	IDENTIFIER
Cy3-AffiniPure Donkey Anti-Rabbit IgG (H+L)	Jackson ImmunoResearch	Cat# 711-165-152; RRID:AB_2307443
Cy3-AffiniPure Donkey Anti-Mouse IgG (H+L)	Jackson ImmunoResearch	Cat# 715-545-150; RRID:AB_2340846
Cy3-AffiniPure Donkey Anti-Goat IgG (H+L)	Jackson ImmunoResearch	Cat# 705-165-147; RRID:AB_2307351
Alexa Fluor 647 Donkey Anti-Goat IgG (H+L)	Jackson ImmunoResearch	Cat# 705-605-147; RRID:AB_2340437
Alexa Fluor 647 Donkey Anti-Mouse IgG (H+L)	Jackson ImmunoResearch	Cat# 715-605-150; RRID:AB_2340862
Alexa Fluor 647 Donkey Anti-Rabbit IgG (H+L)	Jackson ImmunoResearch	Cat# 711-605-152; RRID:AB_2340624
anti-p-JNK	Beyotime Technology	Cat# AM516
Chemicals, Peptides, and Recombinant Proteins		
Tocriscreen TM Total	Tocris	Cat# 2884
Protein Kinase Inhibitor Library I, II, III	Millipore	Cat# 539744; 539745; 539746; 539747
Nuclear Receptor Ligand Library	Enzo	Cat# BML-2802-0500
StemSelect Small Molecule Regulators	Calbiochem	Cat# 56-974-41EA
Selected Small Molecules	This study	N/A
Recombinant Human LIF	Peprotech	Cat# 300-05
Recombinant Human FGF-basic (154 a.a.)	Peprotech	Cat# 100-18B
CHIR 99021	Tocris	Cat# 4423
PD 0325901	Tocris	Cat# 4192
Y-27632 dihydrochloride	Tocris	Cat# 1254
(S)-(+)-Dimethindene maleate	Tocris	Cat# 1425
Forskolin	Tocris	Cat# 1099
Minocycline, Hydrochloride	Santa Cruz Biotechnology	Cat# sc-203339
SB 431542	Tocris	Cat# 1614
IWR-1-endo	Selleckchem	Cat# S7086
Bovine Serum Albumin	Sigma-Aldrich	Cat# A1470
KnockOut Serum Replacement	Thermo Fisher Scientific	Cat# A3181502
ES Screened Fetal Bovine Serum	Hyclone	Cat# SH30070.03E
Fetal Bovine Serum	Hyclone	Cat# SH30396.03HI
Neurobasal Medium	Thermo Fisher Scientific	Cat# 21103-049
DMEM/F-12	Thermo Fisher Scientific	Cat# 11330-032
N-2 Supplement	Thermo Fisher Scientific	Cat# 17502-048
B-27 Supplement, minus vitamin A	Thermo Fisher Scientific	Cat# 12587-010
GlutaMAX	Thermo Fisher Scientific	Cat# 35050-061
Non-Essential Amino Acids Solution	Thermo Fisher Scientific	Cat# 11140-050
2-Mercaptoethanol	Thermo Fisher Scientific	Cat# 21985-023
Penicilin-Streptomycin	Thermo Fisher Scientific	Cat# 15140-122
Mitomycin C from Streptomyces caespitosus	Sigma-Aldrich	Cat# M4287
Trypsin-EDTA (0.05%), phenol red	Thermo Fisher Scientific	Cat# 25300-062
DMEM-Dulbecco's Modified Eagle Medium, High Glucose	Thermo Fisher Scientific	Cat# 11965-092
IMDM-Iscove's Modified Dulbecco's Medium	Thermo Fisher Scientific	Cat# 12440-053
KnockOut DMEM	Thermo Fisher Scientific	Cat# 10829-018
Phosphate-Buffered Saline (PBS)	Corning	Cat# 21-040-CVR
Accutase cell detachment solution	Millipore	Cat# SCR005
Protease from Streptomyces griseus	Sigma-Aldrich	Cat# P8811
G-2 PLUS Medium	Vitrolife	Cat# 10132
Mineral Oil	Sigma-Aldrich	Cat# M8691

(*Continued on next page*)

Continued

REAGENT or RESOURCE	SOURCE	IDENTIFIER
EmbryoMax KSOM Embryo Culture	Millipore	Cat# MR-020P-5F
EmbryoMax M2 medium	Millipore	Cat# MR-015-D
Triton X-100	Sigma-Aldrich	Cat# T8787
Trizol (TRI) Reagent	Sigma-Aldrich	Cat# T9424
Normal Donkey Serum	Jackson ImmunoResearch	Cat# 017-000-121
Paraformaldehyde	DingGuo	Cat# AR-0211
DAPI	Roche Life Science	Cat# 10236276001
Collagenase, Type IV, powder	Thermo Fisher Scientific	Cat# 17104019
Dispase II, powder	Thermo Fisher Scientific	Cat# 17105041
TWEEN 20	Sigma-Aldrich	Cat# P1379
Tripelennamine HCl	Selleckchem	Cat# S3146
Desloratadine	Selleckchem	Cat# S4012
BSI 201	Tocris	Cat# 5817
Nicotinamide	Tocris	Cat# 4106
SB 203580	Tocris	Cat# 1202
SP 600125	Tocris	Cat# 1496
Matrigel matrix	Corning	Cat# 354248
Leukemia Inhibitory Factor, recombinant human	Millipore	Cat# LIF1050
Critical Commercial Assays		
4D-Nucleofector System	Lonza	Cat# AAF-1002B; AAF-1002X; AAF-1002Y
P3 Primary Cell 4D-Nucleofector Kit L	Lonza	Cat# V4XP-3024
RNeasy Mini Kit	QIAGEN	Cat# 74106
QIAquick PCR Purification Kit	QIAGEN	Cat# 28104
Dual-Luciferase Reporter Assay System	Promega	Cat# E1960
DNeasy Blood & Tissue Kit	QIAGEN	Cat# 69506
Power SYBR Green PCR Master Mix	Applied Biosystems	Cat# 4367659
KAPA SYBR FAST Universal 2x qPCR Master Mix	KAPA Biosystems	Cat# KK4601
Halt Protease and Phosphatase Inhibitor Single-Use Cocktail, EDTA-Free	Thermo Fisher Scientific	Cat# 78443
Halt Phosphatase Inhibitor Single-Use Cocktail	Thermo Fisher Scientific	Cat# 78428
2x EasyTaq PCR SuperMix	Transgen Biotech	Cat# AS111
TransScript First-Strand cDNA Synthesis SuperMix	Transgen Biotech	Cat# AT301
NEBNext Ultra DNA Library Prep Kit for Illumina	NEB England BioLabs	Cat# E7370S
NEBNext Ultra RNA Library Prep Kit for Illumina®	NEB England BioLabs	Cat# E7530L
BioCoat Matrigel Invasion Chambers with 8.0 μm PET Membrane in two 24 Well Plates, 12/Pack, 24/Case	Corning	Cat# 354480
Immobilon-P Membrane, PVDF, 0.45 μm	Millipore	Cat# IPVH07850
RNase-Free DNase Set	QIAGEN	Cat# 79254
TransScript One-Step gDNA Removal and cDNA Synthesis SuperMix	Transgen Biotech	Cat# AT311
NuPAGE Novex 10% Bis-Tris Gel	Thermo Fisher Scientific	Cat# NP0315BOX
NuPAGE Novex 12% Bis-Tris Gel	Thermo Fisher Scientific	Cat# NP0341PK2
NuPAGE Transfer Buffer (20X)	Thermo Fisher Scientific	Cat# NP0006
NuPAGE MOPS SDS Running Buffer (for Bis-Tris Gels only) (20X) (500 ml)	Thermo Fisher Scientific	Cat# NP0001

(*Continued on next page*)

Continued

REAGENT or RESOURCE	SOURCE	IDENTIFIER
BeyoECL Star	Beyotime Technology	Cat# P0018A
RIPA lysis buffer	Beyotime Technology	Cat# P0013B
Deposited Data		
RNA-seq data & ChIP-seq data	This study	GEO: GSE89303
Experimental Models: Cell Lines		
H1 (WA01)	WiCell	NIH: hESC-10-0043
H9 (WA09)	WiCell	NIH: hESC-10-0062
0227E	This study	N/A
HSF1	Gift from Kehkooi Kee	NIH: UC01
HSF6	Gift from Kehkooi Kee	NIH: UC06
Primary human embryonic fibroblast	This study	N/A
Primary mouse embryonic fibroblast	This study	N/A
TT2	RIKEN BioResource Center	Stock No.: AES0014
Cell lines established in this study are summarized in Table S2	This study	N/A
Experimental Models: Organisms/Strains		
C57BL/6J-Tg(GOFGFP)11Imeg/Rbrc(OG) mice	RIKEN BioResource Center	Stock No.: RBRC00771
C57BL/6(C57) mice	Beijing Vital River Laboratory Animal Technology	Stock No.: 213
ICR mice	Beijing Vital River Laboratory Animal Technology	Stock No.: 201
129 mice	Beijing Vital River Laboratory Animal Technology	Stock No.: 217
DBA2 mice	Beijing Vital River Laboratory Animal Technology	Stock No.: 214
NPG (NOD-Prkdc^{scid} Il2rgtm1/Vst mice	Beijing Vitalstar Biotechnology	Stock No.: VS-AM-001
B6.Tg(Sox2-cre)1Amc/J mice	The Jackson Laboratory	Stock No.: 008454
B6.Cg-Gt (ROSA) 26Sor$^{tm14(CAG-Tdtomato)Hze}$/J mice	The Jackson Laboratory	Stock No.: 007914
Oligonucleotides		
Oligonucleotides are summarized in Table S6	This study	N/A
Recombinant DNA		
pGL4.74 [hRluc/TK]	Promega	Cat# E6921
pGL3-human OCT4 DE-SV40-Luc	Addgene	Cat# 52414
pCXLE-hOCT3/4	Addgene	Cat# 27076
pCXLE-hSK	Addgene	Cat# 27078
pCXLE-hUL	Addgene	Cat# 27080
pCXLE-EGFP	Addgene	Cat# 27082
Px330-U6-Chimeric_BB-CBh-hSpCas9	Addgene	Cat# 42230
Software and Algorithms		
UltraVIEW VoX system	PerkinElmer	N/A
Volocity	PerkinElmer	http://www.perkinelmer.com.cn/pages/020/cellularimaging/products/volocity.xhtml?utm_source=instrumentDotComNews&utm_campaign=Volocity6_Bio_2011CN
ImageXpress Micro High Content Screening System	Molecular Devices	https://www.moleculardevices.com/systems/high-content-imaging/imagexpress-micro-confocal-high-content-imaging-system

(*Continued on next page*)

Continued

REAGENT or RESOURCE	SOURCE	IDENTIFIER
FlowJo	Ashland	http://www.ashlandchamber.com/ChamberDirectoryDetail.asp?MemberID=2761&CID=284
Bio RAD CFX Connect Real-Time System	BioRAD	http://www.bio-rad.com/en-us/product/cfx-connect-real-time-pcr-detection-system
LSM 710 NLO & DuoScan System	Zeiss	N/A
ZEN 2009	Zeiss	https://www.zeiss.com/microscopy/int/downloads/zen.html
ImageJ	NIH	https://imagej.nih.gov/ij/
Prism 6	GraphPad Software	https://www.graphpad.com
DESeq2	Love et al., 2014	https://bioconductor.org/packages/release/bioc/html/DESeq2.html
Tophat	Trapnell et al., 2009	https://ccb.jhu.edu/software/tophat/index.shtml
BWA	Li and Durbin, 2009	http://bio-bwa.sourceforge.net/
DAVID Bioinformatics Resources 6.7	Huang et al., 2009a, 2009b	https://david-d.ncifcrf.gov/
R version 2.5.0	The R Foundation for Statistical Computing	https://www.r-project.org/
Picard (version 2.6)	Broad Institute	https://broadinstitute.github.io/picard/
ngsplot	Shen et al., 2014	https://github.com/shenlab-sinai/ngsplot
EaSeq	Lerdrup et al., 2016	http://easeq.net/
MACS2 2.1.0	Zhang et al., 2008	https://github.com/taoliu/MACS

CONTACT FOR REAGENT AND RESOURCE SHARING

Further information and requests for resources and reagents should be directed to and will be fulfilled by the Lead Contact, Hongkui Deng (hongkui_deng@pku.edu.cn).

EXPERIMENTAL MODEL AND SUBJECT DETAILS

Small-Molecule Libraries

The small molecule libraries that were used for the screening were purchased or generated in-house as described in Table S1.

Mice

All animal procedures were performed according to NIH guidelines. All of the mouse work performed in Hongkui Deng's laboratory were approved by the Institutional Animal Care and Use Committee of Peking University. All of the mouse work performed in Izpisua Belmonte lab were approved by the Salk Institute Institutional Animal Care and Use Committee. C57BL/6J-Tg (GOFGFP) 11Imeg/Rbrc (OG) mice (Stock No.: RBRC00771) were obtained from RIKEN BioResource Center. C57BL/6 (C57), ICR, 129, and DBA2 mice were obtained from Beijing Vital River Laboratory Animal Technology Co., Ltd. NOD-Prkdc^{scid} Il2rgtm1/Vst (NPG) mice were obtained from Beijing Vitalstar Biotechnology. B6.Tg (Sox2-cre) 1Amc/J (Stock No.: 008454) and B6.Cg-Gt (ROSA) 26Sor$^{tm14(CAG-Tdtomato)Hze}$/J (Stock No.: 007914) mice were obtained from The Jackson Laboratory. Experiments with OG, C57, ICR, F1 hybrids between B6.Tg(Sox2-cre)1Amc/J and B6.Cg-Gt(ROSA)26Sor$^{tm14(CAG-Tdtomato)Hze}$/J, F1 hybrids between C57 and 129, F1 hybrids between DBA2 (male) and C57 (female), F1 hybrids between C57 and 129 mice were performed in females at 7-8 weeks of age. Experiments with NPG mice were performed in males at 8 weeks of age. For chimeric experiments, mouse embryos and conceptuses at embryonic day E2.5, E3.5, E6.5, E7.5, E10.5, E12.5, E13.5, and E17.5 were used or analyzed. For embryo microinjections, mouse embryos were randomly selected for injecting with different pluripotent cell types. Any animals that appeared unhealthy before the start of experiments were excluded. No inclusion criterion was used. The mice were housed with a 12 hr light/dark cycle between 06:00 and 18:00 in a temperature controlled room (22 ± 1°C) with free access to water and food.

Human Samples

Human embryonic fibroblasts were isolated from 2- to 3-month-old embryos that were obtained with informed written consent and approval by the Clinical Research Ethics Committee of China-Japan Friendship Hospital (No. 2009-50). The establishment of induced pluripotent stem cells with donated human fibroblasts was approved by the Ethics Committee of Peking University

Health Science Center (IRB00001052-08093). Human embryos at the blastocyst stage produced by in vitro fertilization for clinical purposes were obtained with informed written consent and approval from the Ethics Committee of Peking University Health Science Center (IRB00001052-08091) and Stem Cell Research Oversight of Peking University (SCRO201101). The cross-species chimeric experiments performed in Deng lab were reviewed and approved by the Ethics Committee of Peking University Health Science Center (LA2014230) and followed the ethical guidelines for human embryonic stem cell research released by the International Society for Stem Cell Research (ISSCR). All the chimeric experiments performed in Izpisua Belmonte lab were reviewed and approved by the Stem Cell Research Oversight Committee (SCRO# 1127) and followed the ethical guidelines of the Salk Institute.

Culture of Mouse Embryos

During the process of injection, mouse 8-cell embryos were placed in drops of EmbryoMax M2 medium (Millipore, MR-015-D) covered with Mineral oil (Sigma-Aldrich, M8691). After injection, the embryos were transferred into drops of EmbryoMax KSOM Embryo Culture (Millipore, MR-020P-5F) or G-2^{TM} PLUS medium (Vitrolife, 10132) in a humidified incubator under 5% CO_2 at 37°C.

Culture of Human and Mouse EPS Cells

Human and mouse EPS cells were cultured in serum-free N2B27-LCDM medium under 20% O_2 and 5% CO_2 at 37°C. A total of 500 mL of N2B27 medium was prepared by including: 240 mL DMEM/F12 (Thermo Fisher Scientific, 11330-032), 240 mL Neurobasal (Thermo Fisher Scientific, 21103-049), 2.5 mL N2 supplement (Thermo Fisher Scientific, 17502-048), 5 mL B27 supplement (Thermo Fisher Scientific, 12587-010), 1% GlutaMAX (Thermo Fisher Scientific, 35050-061), 1% nonessential amino acids (Thermo Fisher Scientific, 11140-050), 0.1 mM β-mercaptoethanol (Thermo Fisher Scientific, 21985-023), penicillin-streptomycin (Thermo Fisher Scientific, 15140-122), 5 mg/ml BSA (Sigma-Aldrich, A1470, optional) or 5% knockout serum replacement (KSR, Thermo Fisher Scientific, A3181502, optional). Small molecules and cytokines were purchased from Peprotech, Tocris, Santa Cruz, Selleckchem, and Sigma-Aldrich. To prepare the N2B27-LCDM medium, small molecules and cytokines were added in the N2B27 medium as indicated at the following final concentrations: 10 ng/ml recombinant human LIF (L, 10ng/ml; Peprotech, 300-05), CHIR 99021 (C, human: 1 μM, mouse: 3 μM; Tocris, 4423), (S)-(+)-Dimethindene maleate (D, 2 μM; Tocris, 1425) and Minocycline hydrochloride (M, 2 μM; Santa Cruz Biotechnology, sc-203339). For human EPS cell culture, the addition of IWR-endo-1 (0.5-1 μM; Selleckchem, S7086) and Y-27632 (2 μM; Tocris, 1254) was recommended. Human and mouse EPS cells were cultured on mitomycin C (Sigma-Aldrich, M4287) inactivated mouse embryonic fibroblast (MEF) feeder cells (3*10^4 cells per cm^2). The N2B27-LCDM medium was changed every day with fresh LCDM medium. To maintain human EPS cells in an undifferentiated state, we used the following criteria: a) avoid plating human EPS cells too sparsely; b) use the proper quantity of freshly prepared MEF feeder cells; and c) do not allow human EPS cells to overgrow. EPS cells were passaged by single-cell trypsinization (0.05% trypsin-EDTA, Thermo Fisher Scientific, 25300-062) every 2–4 days (normally at a split ratio ranging from 1:3 to 1:10), and the exact passage day and split ratio should be determined for each cell line specifically. Passage numbers of the EPS cells indicated the number of passages counted after the acquirement of the extended pluripotent state.

Culture of Primed hPSCs

The following already established primed hPSC lines were used (the passage number of the cell line taken for EPS conversion is indicated in parentheses): H1 (around passage 30), H9 (around passage 40), 0227E (around passage 20), HSF1 (around passage 50) and HSF6 (around passage 60). The cell lines H1 (WA01, NIHhESC-10-0043) and H9 (WA09, NIHhESC-10-0062) were obtained from WiCell and were authenticated by karyotype analysis. The 0227E cell line was established in our laboratory. The HSF1 (NIH code UC01) and HSF6 (NIH code UC06) cell lines were kindly provided by Kehkooi Kee (Department of Basic Medical Sciences, School of Medicine, Tsinghua University).

Primed hPSCs were cultured under 20% O_2 and 5% CO_2 at 37°C condition on mitomycin C-inactivated mouse embryonic fibroblast (MEF) feeder cells (2*10^4/cm^2) in conventional hPSC medium. The formulation of hPSC medium includes: DMEM/F12 supplemented with 20% knockout serum replacement (KSR), 1% GlutaMAX, 1% nonessential amino acids, 0.1 mM β-mercaptoethanol, and 4-10 ng/ml bFGF (Peprotech, 100-18B). To maintain primed hPSCs in an undifferentiated state before conversion, it is recommended that the feeder cells be freshly prepared one day before the passage of primed hPSCs. Primed hPSCs are routinely passaged at a split ratio of 1:3 to 1:5 using Dispase II (Thermo Fisher Scientific, 17105-041) every 5-7 days.

Culture of Mouse Naive ES Cells

Mouse naive ES cells were maintained under 20% O_2 and 5% CO_2 at 37°C on mitomycin C-inactivated MEF feeder cells (3*10^4/cm^2) or gelatin-coated dishes, in 2i medium that contained serum-free N2B27 medium supplemented with 10 ng/ml hLIF, 3 μM CHIR 99021 and 1 μM PD 0325901 (Tocris, 4192). Cells were passaged every 2-4 days using 0.05% trypsin-EDTA. TT2 mouse ES cell line (Stock No.: AES0014) was obtained from RIKEN BioResource Center.

METHOD DETAILS

Chemical Screening

To screen for small molecules that activate *OCT4* DE, primed hPSC cells (H9) were dissociated in Accutase (Millipore, SCR005). Then, *OCT4*-DE luciferase plasmid (Addgene, 52414) was transfected into H9 cells by nucleofection (4D-Nucleofector System,

Lonza). A control vector pGL4.74 [hRluc/TK] (Promega, E6921) was co-transfected for normalization. After transfection, H9 cells were seeded into Matrigel (Corning, 354248) coated 24-well plates at a density of $2*10^4$ cells per well and cultured in conventional hPSC medium (DF12 plus 20% KSR, detailed formulation is provided above) plus 10 μM Y-27632. 12 hr later, the medium was replaced with N2B27 medium supplemented with hLIF and 2i (10 ng/ml hLIF, 1 μM MEK inhibitor PD 0325901, and 3 μM GSK3β inhibitor CHIR 99021) (detailed formulation of N2B27 medium is provided above). One single compound from the libraries was added into each well. After being treated for 6 days, the H9 cells were lysed for detecting the luciferase activity using the Dual-Luciferase Reporter Assay System (Promega, E1960). After the screening, more than 100 candidates were obtained, which could enhance the *OCT4* DE activity by more than 2-fold compared with cells that were cultured in conventional primed hPSC medium.

To further identification of small molecules that support dome-shaped human ES colony formation, H9 cells were digested into single cells using Accutase and were seeded into a matrigel-coated 24-well plate ($2*10^4$ cells per well) on day 0 in conventional hPSC medium supplemented with 10 μM Y-27632. The next day, the conventional hPSC medium was replaced by the N2B27 medium supplemented with the hLIF+2i base, and candidates from the first round of screening were added individually into each well. The medium was changed every 2 days. Then, 6 days later, a TGFβ inhibitor SB 431542 (10 μM; Tocris, 1614) was added into the wells that contained un-differentiated cells for another 6 days. After the screening, more than 30 candidates were obtained that supported TGFβ-signaling-independent self-renewal in the short term.

Combination and Optimization of the LCDM Condition

Individual candidate was combined with 2i plus hLIF for culturing hPSCs in the long term. After 3-5 passages, for most candidates, treated hPSCs gradually differentiated or cannot well maintain the domed shape. However, wells treated by MiH still contained domed colonies. To further find the optimal conditions for maintaining domed hPSC colonies in long term, the rest of candidates were individually added into the base containing 2i, MiH and hLIF. After 10-20 passages, DiM was found to well-maintain the domed colonies under such condition. This screening was performed in three primed human ES cell lines, including H1, H9 and 0227E. After further optimization, we found that PD 0325901 was dispensable for the self-renewal of hEPS cells, and fine tuning of the concentration of CHIR 99021 could promote EPS colony formation (higher concentration of CHIR 99021 may cause spontaneous differentiation of hEPS cells).

Conversion of Primed hPSCs into hEPS Cells

Conversion was usually conducted on day 3 or day 4 after the passage of primed hPSCs (primed hPSCs were usually passaged every 5-6 days in our laboratory), and hPSC colonies usually reached 60%–70% of confluence. Mitomycin C-inactivated mouse embryonic fibroblast (MEF) feeder cells were seeded ($3*10^4$ cells per cm^2) one day before the conversion. Small molecules and cytokines (purchased from Peprotech, Tocris, Selleckchem, or Santa Cruz) were supplemented as indicated at the following final concentrations: hLIF: 10 ng/ml; CHIR 99021: 1 μM; (S)-(+)-Dimethindene maleate (DiM): 2 μM; Minocycline hydrochloride (MiH): 2 μM. For deriving and culturing hEPS cell lines with different genetic backgrounds, the concentration of CHIR, DiM and MiH may need re-optimized. It is also recommended that IWR-1-endo (0.5-1 μM) and Y-27632 (2 μM) are added into the N2B27-LCDM medium: IWR-1-endo could inhibit the spontaneous differentiation effect induced by the dosage effect of CHIR 99021 treatment in specific human EPS cell lines, and low concentrations of Y-27632 treatment promote human EPS cell proliferation. To prepare the stock solutions, small molecules were dissolved in DMSO and stored at −20°C, and human LIF was dissolved in 0.1% BSA solution (use 1xPBS to dissolve BSA) and stored at −20°C. Once used, the rest of stocked small molecules and cytokines could be stored at 4°C for up to 1 week. Prepared LCDM medium could be kept at 4°C for up to 1 week.

To digest primed hPSCs for conversion, the conventional hPSC medium was removed from the well of cells, and DMEM/F12 medium was used to wash primed hPSCs to ensure that no dead cells or cell debris remained in the culture. Then, the DMEM/F12 medium was removed and Dispase II was added. The cells were incubated at 37°C in the incubator for 5-10 min, and then, the Dispase solution was aspirated. The cells were further washed using DMEM/F12 medium. After that, DMEM/F12 medium was added, and the cells were washed off of the surface of the dish by pipetting the medium slowly up and down. The large primed hPSC colonies were broke into small clumps at this time. Cells were collected in an appropriately sized tube and centrifuged at 800 rpm (200 xg) at room temperature for 3 min. The supernatant of the centrifuged cells was carefully removed. The cells were re-suspended in an appropriate volume of conventional hPSC medium (according to the cell lines and growth ratio). The small colonies were seeded to the plate with MEF feeders. The split ratio was usually from 1:3 to 1:10. Then, the cells were incubated under 20% O_2, 5% CO_2 at 37°C. Optionally, if primed hPSCs were tolerant to single cell digestion after Y-27632 (10 μM) treatment, then the primed hPSCs could be digested into single cells using 0.05% Trypsin-EDTA. Y-27632 (10 μM) was recommended to be added to the medium during the first 12 hr after passaging.

Subsequently, 12 hr after seeding, the conventional hPSC medium was replaced with the N2B27-LCDM medium (addition of IWR-endo-1 (0.5-1 μM) and Y-27632 (2 μM) was recommended). The N2B27-LCDM medium was changed daily. Dome-shaped colonies gradually emerged during this period. Then, 3-6 days later, 0.05% Trypsin-EDTA was used to trypsinize the cells for 3 min at 37°C in the incubator. MEF medium was used to stop the trypsinization. The cells were washed off the surface of dish by pipetting the medium slowly up and down: they were collected in an appropriately sized tube and centrifuged at 1, 200-1, 600 rpm (250-450 xg) at room temperature for 3 min. The cells were re-suspended in an appropriate volume of N2B27-LCDM medium (according to the cell lines and growth ratio) and seeded into the plate with MEF feeders. For one six-well plate, approximately 50,000-100,000 cells per

well were seeded. The split ratio was usually from 1:3 to 1:10. Then, the cells were incubated under 20% O_2 and 5% CO_2 at 37°C. If the cells grow slowly after the single-cell passage, then it is recommended to lower the split ratio (from 2:1 to 1:3) during the first few passages (3-5 passages). After a few passages, cells that were cultured in the LCDM medium could gradually proliferate well.

For the chimeric experiment, primed hPSC-derived hEPS cells with higher passages (passage > 10 after conversion) were recommended to be used to ensure that the hEPS cells were reprogrammed to the extended pluripotent state. In our hand, converted domed colonies at passage 10 showed bi-potentiality in chimeric experiments. The conversion of human primed PSCs into hEPS cells was repeated by six different colleagues in the Hongkui Deng's laboratory in at least 20 independent experiments, which was also independently validated by the Juan Carlos Izpisua Belmonte's laboratory.

Human EPS Cell Derivation from Blastocysts

Whole embryos were seeded onto mitomycin C-inactivated MEF feeder cells ($4*10^4/cm^2$). The MEF medium was changed into the FBS-LCDM medium at least half an hour before the embryos were seeded. The FBS-LCDM medium was prepared by including: KnockOut DMEM (Thermo Fisher Scientific, 10829-018) supplemented with 10% knockout serum replacement (KSR), 10% ES Screened Fetal Bovine Serum (Hyclone, SH30070.03E), 1% GlutaMAX, 1% nonessential amino acids, and 0.1 mM β-mercaptoethanol. Small molecules and cytokines (purchased from Peprotech, Tocris or Santa Cruz) were supplemented as indicated at the following final concentrations: hLIF: 10 ng/ml; CHIR 99021: 1 μM; (S)-(+)-Dimethindene maleate (DiM): 2 μM; Minocycline hydrochloride (MiH): 2 μM. To enhance the survival of embryo, Y-27632 (10 μM) was recommended to be added into the FBS-LCDM medium.

For the unhatched blastocysts, the zona pellucida was removed by protease (Sigma-Aldrich, P8811). The time for the treatment of protease varied among different blastocysts, which is generally from 0.5 min to 5 min. It would be helpful to gently blow up and down the blastocyst during treatment. When the zona pellucida began to disappear, the blastocysts were transferred into the G-2™ PLUS medium (Vitrolife, 10132) that was prepared earlier as soon as possible. The embryos were washed 3 to 5 times to remove the residual protease, and then, they were seeded onto the prepared MEF feeder. Two days later, the FBS-LCDM medium was changed into N2B27-LCDM medium if the embryo had attached onto the MEF feeder. Otherwise, half of the cultured FBS-LCDM medium was removed and changed into the N2B27-LCDM medium. Initial outgrowths became visible about 4 to 7 days after being seeded and were dissociated mechanically into small clumps. Then, the cells were reseeded on the MEF feeder cells with the FBS-LCDM medium.

During the first few passages (3-5 passages), it was recommended to dissociate the colonies mechanically and culture them in the FBS-LCDM medium supplemented with Y-27632 (10 μM) for the first 2 days after seeding. The FBS-LCDM medium was changed into the N2B27-LCDM medium later. Colonies morphologically resembled mouse ES colonies gradually emerged. If these colonies survived and proliferated well, 0.05% trypsin-EDTA could be used for digesting cells. The newly established cell lines were further passaged using 0.05% trypsin-EDTA, and then, they were either frozen or used for further analysis.

hEPS Generation by Reprogramming Somatic Cells

For reprogramming with oriP/EBNA1-based episomal vectors, episomal plasmids including pCXLE-hOCT3/4, pCXLE-hSK, pCXLE-hUL and pCXLE-EGFP (Addgene 27076, 27078, 27080, 27082) were co-transfected into human embryonic fibroblasts via nucleofection (4D-Nucleofector System, Lonza). Transfected fibroblasts (approximately $1*10^6$ cells per nucleofection) were directly plated into three 10-cm feeder-seeded dishes in Dulbecco's modified Eagle's medium (Thermo Fisher Scientific, 11965-092), which contained 10% fetal bovine serum (Hyclone, SH30396.03HI). The fibroblasts were re-plated 7 days post-infection and cultured in Knockout DMEM (Thermo Fisher Scientific, 11965-092) with 10% fetal bovine serum and 10% KSR containing 10 ng/ml bFGF, 3 μM CHIR 99021, 10 ng/ml human LIF, 10 μM Forskolin (Tocris, 1099). The culture medium was changed every other day. On day 12 post-transfection, the medium was replaced with the N2B27-LCDM medium. Colonies that morphologically resemble EPS colonies became gradually visible on day 15 after transfection. The colonies were picked and passaged by 0.05% trypsin-EDTA for further analysis.

Establishment and Culture of Mouse EPS Cells

mEPS cells were derived directly from blastocysts of OG, C57, or F1 hybrids between B6.Tg(Sox2-cre)1Amc/J and B6.Cg-Gt(ROSA)26Sor$^{tm14(CAG-Tdtomato)Hze}$/J, or F1 hybrids between C57 and 129 mice. Blastocysts were seeded onto MEF feeders with N2B27-LCDM medium. Then, 4 days later, outgrowths were observed and dissected into small clumps. mEPS cells were passaged every 2-3 days and frozen or used for further analysis. For the mEPS cells that were converted directly from mouse naive ES cells TT2 cultured using the 2i medium (TT2-2i), the 2i medium was replaced with N2B27-LCDM medium 12 hr after seeding. Then, 2-3 days later, the colonies were passaged for further analysis.

Chimeric Assay of Multiple-Cell Microinjection

The cross-species chimeric assay was approved by the Ethics Committee of Peking University Health Science Center (LA2014230). All the chimeric experiments performed in Izpisua Belmonte lab were reviewed and approved by the Stem Cell Research Oversight Committee (SCRO# 1127) and followed the ethical guidelines of the Salk Institute. For chimeric experiments, human and mouse EPS cells were used one day before passaging, which showed an optimal undifferentiated morphology and proliferated

exponentially. At this time point, the colonies should be at sub-confluent density (approximately 70% density of the day cells should be passaged).

For hEPS cell injection, hEPS cells were first trypsinized by 0.05% trypsin-EDTA, and the digested cells were filtered through a cell strainer (40 μm). Afterward, the cells were centrifuged at 1, 200-1, 500 rpm (250-390 × g) at room temperature for 3 min. Supernatant was removed, and the cells were re-suspended in the culture medium at a proper density (2-6*10^5 cells/ml). 10 μM Y-27632 was recommended to be added into the suspension. The suspension was placed on ice for 20-30 min before injection. 10-15 of the digested cells were microinjected into each E2.5 (recommended) or E3.5 embryo of ICR or C57 diploid mouse embryo. Approximately 15 injected embryos were transferred to each uterine horn of 0.5 or 2.5 day post-coitum pseudo-pregnant ICR females.

For the injection of mEPS cells and naive mouse ES cells, the cells were trypsinized and microinjected in the same way as the hEPS cells except that Y-27632 was not added into the suspension. Occasionally, several pregnant mice were excluded from further analysis on conditions that no mouse embryos were obtained from those mice.

Chimeric Assay of Single-Cell Microinjection

The cells used in this experiment were cultured and prepared in a way that was similar to that of the multiple-cell microinjections. The cell suspension was placed on ice for 20-30 min before injection. After being placed on ice, the digested single cells were used for injection within 1 hr: in other words, the whole injection process should not take more than 30 min. If the cells were placed on ice for more than 1 hr, then another batch of cells was digested for the remaining injections. The injection was performed with the assistance of XY Clone laser (Hamilton Thorne, Inc.). Single cells were microinjected into 8-cell stage ICR diploid mouse embryos. The time that the embryos are exposed to room temperature should not exceed 30 min. Afterward, the injected embryos are recovered for 1-2 hr in a humidified incubator with 5% CO_2 at 37°C.

It is important to ensure that the injected single cell is not pushed out while the needle is being withdrawn. To achieve this goal, we usually attempt to use the injection needle to gently press the zona pellucida so that the blastomeres could move to the position near the pore in the zona pellucida, which would minimize the possibility that the single injected cell is pushed out from the pore. For single cells that are labeled with a fluorescent reporter, it is recommended that all of the injected embryos are checked under the fluorescence microscope to ensure that each individual embryo is injected with a single cell. For the generation of chimeric blastocysts, the injected embryos were cultured in the N2B27-LCDM medium for the first 4 hr (10 μM Y-27632 was recommended to be added for the culture of chimeric embryos injected with single hEPS cells), and then, they were changed into the G-2^{TM} PLUS medium. After 48-60 hr, the embryos were fixed and immunostained.

For the generation of single mEPS cell-derived in vivo chimeric conceptuses, chimeric embryos that were injected with single mEPS cells were recovered for 1-2 hr in a humidified incubator under 5% CO_2 at 37°C and were transferred to uterine horns of 0.5 day post coitum pseudo-pregnant females. The conceptuses were dissected at the E10.5, E12.5 or E17.5 developmental stages and observed using an immunofluorescence stereomicroscope for detecting Tdtomato$^+$ cell localization. The placenta was isolated from the E10.5 conceptuses, followed by embedding, freezing, slicing (10 μm thick) from the sagittal side and then, staining with CK8 (1:400; Sigma-Aldrich, HPA049866), PROLIFERIN (1:50; Santa Cruz, sc-47345) or TPBPA (1:100; Abcam, ab104401). The samples were further analyzed by the ImageXpress Micro High Content Screening System (MolDev).

Detection of hEPS Derivatives in Mouse Conceptuses

Conceptuses were dissected at the E10.5 developmental stage. For whole-mount staining, an anti-human nuclei antibody (clone 235-1, 1:300; Millipore, MAB1281) was co-stained with anti-GATA4 (1:200; Santa Cruz, sc-1237) or anti-SOX2 (1:200; Santa Cruz, sc-17320) antibodies according to the whole-mount staining protocol from Abcam. Then the mounted embryos were imaged by the UltraVIEW VoX system (PerkinElmer) from the sagittal side.

For immunostaining of tissue sections, embryos and placentas were isolated from the E10.5 conceptuses. For NANOG detection, the embryos were embedded, frozen and sliced (10 μm thick) from the sagittal side. The embryos which were injected with Tdtomato-labeled human cells were stained with an anti-NANOG (1:200; Abcam, ab80892) antibody. The placentas were sliced (10 μm thick) from the sagittal side and co-stained with anti-Tdtomato/RFP (1:1000; Biorbyt, orb182397) and anti-CK8 (1:400; Sigma-Aldrich, HPA049866). All these samples were imaged by the ImageXpress Micro High Content Screening System (MolDev).

Derivation of TS- and ES-like Cells

A single Tdtomato-labeled mEPS cell was injected into an 8-cell mouse embryo and cultured in the N2B27-LCDM medium for 4 hr. The injected embryos were transferred to G-2^{TM} medium and cultured for additional 56 hr. The same chimeric embryos were used to generate both ES and TS cell lines by seeding half of the embryos into mES derivation medium (2i+hLIF) while the other half were seeded into conventional TS derivation medium (Tanaka et al., 1998). Both ES- and TS-like colonies were derived from the same chimeric embryo simultaneously. Tdtomato-labeled mouse ES TT2 and mc2i-1 were used as controls in this assay separately: each 8-cell embryo was injected with 10-15 mouse ES cells and cultured for an additional 48–60 hr. The chimeric embryos were seeded into ES or TS derivation medium respectively.

Chimeric Assay of the TS-like and ES-like Cells

10-15 cells of the established TS-like or ES-like cell line were injected into an 8-cell mouse embryo. For the in vivo chimeric assay, the conceptuses were dissected at E13.5 developmental stage and observed using an immunofluorescence stereomicroscope for detecting the presence of fluorescent positive cells.

Immunofluorescence

The cells were fixed in 4% paraformaldehyde (DingGuo, AR-0211) at room temperature for 15 min and blocked with PBS (Corning, 21-040-CVR) that contained 0.2% Triton X-100 (Sigma-Aldrich, T8787) and 3% normal donkey serum (Jackson Immuno Research, 017-000-121) at room temperature for 45 min. The cells were incubated with primary antibodies at 4°C overnight. Secondary antibodies (Jackson ImmunoResearch) were incubated at room temperature for 1 hr. The nuclei were stained with DAPI (Roche Life Science, 10236276001). Antibody details were provided below.

For human EPS cells, the following antibodies were used: anti-OCT4 (1:200; Santa Cruz, sc-5279), Anti-trimethyl-Histone H3 (Lys27) (1:300; Millipore, 07-449) and anti-KLF4 (1:200; Santa Cruz, sc-20691). For the immunofluorescent analysis of TS-like cells, ES-like cells or mEPS and mES cells cultured in TS medium, the used antibodies included: anti-OCT4 (1:200; Santa Cruz, sc-5279), anti-NANOG (1:100; Abcam, ab80892), anti-SOX2 (1:200; Santa Cruz, sc-17320), anti-CDX2 (CDX2-88; Biogenex, AM392) and anti-EOMES (1:200; Abcam, ab23345). For mouse EPS cells, the following antibodies were used: anti-NANOG (1:100; Abcam, ab80892), anti-OCT4 (1:200; Abcam, Ab18976), anti-SALL4 (1:500; Abcam, ab29112) and anti-SOX2 (1:200; Santa Cruz, sc-17320). For the immunofluorescent analysis of chimeric blastocysts, the used antibodies included: anti-OCT4 (1:200; Abcam, ab181557), anti-GATA3 (1:200; Santa Cruz, sc-268), anti-NANOG (1:100; Abcam, ab80892) and anti-CDX2 (CDX2-88; Biogenex, AM392).

Flow Cytometry

Chimeric placental tissues were gently isolated and digested into single cells using Collagenase IV (Thermo Fisher Scientific, 17104019). Suspensions were filtered through a cell strainer (40 μm). Then, the samples were analyzed on a BD LSRFortessa machine. Data analysis was performed using FlowJo software (Ashland).

Analysis of Trophoblast Marker Gene Expression

Chimeric placental tissues were isolated and digested using Collagenase IV. Suspensions were filtered through a cell strainer (40 μm). Both primary Tdtomato$^+$ and Tdtomato$^-$ placental cells were purified using FACS. Total RNAs of purified cells was extracted using Trizol (Sigma-Aldrich, T9424). cDNAs were prepared and amplified using the Smart-seq2 approach. The amplified cDNA product was diluted ten-fold as required by the qPCR template. Quantitative PCR analysis was conducted using the KAPA SYBR FAST qPCR Kit (KAPA Biosystems, KK4601) on a Bio RAD CFX Connect Real-Time System. The primers that were used for Q-PCR are listed in Table S7.

DNA Content Analysis of mEPS Placental Derivatives

Chimeric placental tissues were isolated and gently digested using Collagenase IV. Isolated placental cells were fixed in 2% paraformaldehyde at room temperature for 20 min, and stained in DAPI supplemented with Triton X-100 solution (0.1%) at room temperature for 30 min. Suspensions were filtered through a cell strainer (100 μm). Then stained cells were analyzed on a BD LSRFortessa machine. Data analysis was performed using FlowJo software (Ashland). Because the placenta contains mixed cell populations and polyploid trophoblast giant cells generally have larger cell size than other placental cells, placental cells were first gated into two populations basing on their cell sizes. Then Tdtomato-positive cells were further gated for assessing DNA contents as judged by the intensity of DAPI signals.

Transwell-Based Invasive Assay

Chimeric placental tissues were isolated and digested using Collagenase IV. Primary placental cells from one or half of the chimeric placenta were seeded onto Matrigel-coated filters (BioCoat Matrigel® Invasion Chambers, Coring, 354480) in 24-well plates. Briefly, the cells were seeded onto the upper chamber of the Transwell in serum-free DMEM/F12 media. The lower chamber of the Transwell was filled with DMEM/F12 media that contained 10% FBS. The chambers were incubated at 37°C with 5% CO_2 for 24 hr. At the end of the incubation, the cells on the upper surface of the filter were removed using a cotton swab. The cells invading through the filter to the lower surface were fixed with 4% paraformaldehyde for 20 min, and further analyzed by immunofluorescence. The following antibodies were used for immunofluorescence: anti-CK8 (1:50; Santa Cruz, sc-52324) and anti-CK7 (1:40; Thermo Scientific, MA5-11986).

EB Formation Assay

Mouse and human EPS cells were trypsinized to single cells, separated from the MEF feeder cells by pre-plating on gelatin-coated plates, and cultured for 6 days on ultra-low attachment plates in IMDM (Thermo Fisher Scientific, 12440-053) supplemented with 15% FBS. Then, EBs were collected and plated on the Matrigel-coated plates for 6 days in the same medium, fixed and detected. For human cells, antibodies include anti-FOXA2 (1:200; Abcam, ab108422), anti-LHX5 (1:200; Santa Cruz, sc-130469) and

anti-α-SMA (1:400; Millipore, CBL171). For mouse cells, the antibodies included anti-FOXA2 (1:200; ab60721; Abcam), anti-β-III TUBULIN (1:300; Santa Cruz, sc-80016) and anti-α-SMA (1:400; Millipore, CBL171).

Evaluation of hOCT4 Transcriptional Regulation

To evaluate human *OCT4* transcriptional regulation in human cell lines, *OCT4*-DE luciferase plasmid was transfected into cells by nucleofection (4D-Nucleofector System, Lonza). A control vector pGL4.74 [hRluc/TK] was co-transfected for normalization. Baseline activity was analyzed by transfection with an empty vector. After transfection, cell lines were seeded into Matrigel-coated 96-well plates at a density of $5*10^3$ cells per well. Then, 48 hr later, the cells were lysed for detecting luciferase activity using the Dual-Luciferase Reporter Assay System.

Teratoma and Immunochemistry Assay

Human and mouse EPS cells were collected by trypsinization before injection. Approximately 10^6 cells were injected sub-cutaneously into immunodeficient NPG mice. Teratomas generally developed within 2–6 weeks, and the animals were killed before the tumor size exceeded 1.5 cm in diameter. The teratomas were then embedded in paraffin and processed for hematoxylin and eosin staining.

To analyze the ExEm differentiation potential of hEPS cells in teratoma assay, immunochemistry assay was applied. After the hEPS- or primed hPSC-derived teratomas were fixed and embedded, 5-μm-thick sections were used for immunohistochemistry staining. After dewaxation and hydration, 3% H_2O_2 was used to block endogenous peroxidase. Subsequently, the tissues were blocked by 10% normal serum of the secondary antibody animal origin. Samples were incubated with the primary antibody anti-hCGβ (1:100; Abcam, ab131170) at 4°C and further incubated with the second antibody conjugated with horseradish peroxidase (HRP) (ZSGB-BIO, ZDR-5306) for 30 min at room temperature. After visualization by diaminobenzidine (DAB), the tissues were stained with Harris hematoxylin.

Karyotype Analysis

Cell cultures were prepared to give a 50 ± 70% confluence on day of sampling. After 2 hr incubation with fresh medium, a Colcemid solution was added to the medium at a final concentration of 0.02 μg/ml and incubated for 1 hr. Then the cells were washed in PBS, trypsinized and spun down. To obtain a single cell suspension, the pellet was re-suspended in hypotonic solution (0.56% KC1), and left at room temperature for 6 min. After spinning and removing hypotonic solution, 5 mL of ice-cold fixative (3:1 methanol: acetic acid) was added dropwise to the suspension, left at roo temperature for 5 min and then spun down. The fixing procedure was further repeated for additional three times. Finally, the pellet was re-suspended in a final volume of 1 mL fixative. The cells were then dropped onto 5% acetic acid ± ethanol (ice-cold) washed slides and stained with Giemsa. For each analysis, at least 30 ± 40 metaphases were examined. The number of chromosomes as well as the presence of structural chromosomal abnormalities was examined.

Comparative Genomic Hybridization (CGH) Analysis

For CGH experiments, genomic DNA was extracted and hybridized to Custom SurePrint G3 8x60K human whole-genome AGI-CGH arrays by Imagenes using cell lines at early passage as a reference.

Doubling Time Calculation

The cells were removed from the plates using 0.05% trypsin-EDTA, counted and plated onto 24-well plates that were pre-seeded with feeder cells at a density of 10,000 cells per well in the appropriate medium without Y-27632. The growth rate was determined by counting the number of cells using a hemocytometer as a function of time. Data from the exponential phase of growth (time points at 48 and 72 h) were used to obtain an exponential growth curve. The doubling time was calculated following the formula: DT = 48*[$\log_2$/(lgNt(number of cells at day4)-lgNo (number of cells at day2))].

Analysis of Single Cell Cloning Efficiency

Cells were trypsinized, counted using a hemocytometer, and plated onto pre-seeded 6-well plate feeders at a density of 10, 100, 1,000 cells per well in triplicates under LCDM or primed hPSC conditions. Single primed hPSCs were cultured under conventional hPSC medium with or without 10 μM Y-27632 upon passage for the subsequent 24 hr. The colonies were counted 6 days later, and cloning efficiency was assessed as a percentage of colony number per number of cells seeded.

Transcriptome Analysis

Total RNA was isolated from primed hPSCs, hEPS cells, mES cells and mEPS cells using the RNeasy Mini Kit (QIAGEN, 74106). RNA sequencing libraries were constructed using the NEBNext® Ultra RNA Library Prep Kit for Illumina® (NEB England BioLabs, E7530L). The fragmented and randomly primed 2x100-bp paired-end libraries were sequenced using an Illumina HiSeq 2000 (mouse cells) or 2500 (human cells). The generated sequencing reads were mapped against human genome build hg19 for human and GRCm38/mm10 for mouse using TopHat alignment software tools. The read counts for each gene were calculated, and the expression values of each gene were normalized using RPKM (human cells) or FPKM (mouse cells).

To compare EPS cells with other pluripotent cells, the published data of human naive PSCs, human primed PSCs, mouse EpiSCs, mouse 2C-like cells and mouse ES cells were included. Bioinformatic analysis was restricted to the genes interrogated by each

sample. For the expression profile of human reset PSCs, 3iL hESCs, and conventional primed hPSCs published in Takashima et al. (2014) and Chan et al. (2013), raw sequencing reads (E-MTAB-2857) and (E-MTAB-2031) from ArrayExpress database were re-mapped and processed as described above. For the expression profile of human naive PSCs and human primed PSCs published in Gafni et al. (2013) and Theunissen et al. (2014), normalized microarray data under GSE46872 and GSE59430 in the NCBI GEO database were downloaded and merged, respectively. For the expression profile of mouse ES cells (GSM659549, GSM659550) and EpiSCs (GSM659551, GSM659552, GSM659553, GSM659554) published in Najm et al. (2011), the normalized expression tables were downloaded and merged. For the expression profile of 2C-like cells published in Macfarlan et al. (2012), the normalized expression data of 2C::tomato+ cells and 2C::tomato- cells (GSM8351954, GSM8351998) were downloaded and processed in the same manner as described above. The probe sets of the same gene were collapsed into a single value to represent the gene by taking the mean value. To compare EPS cells with embryonic cells from preimplantation stages, the published data of human and mouse embryonic cells at preimplantation stages were used (Tang et al., 2011; Yan et al., 2013). Accounting for the platform and batch effect among the different datasets, the expression values from the published data and our data were recalculated by normalizing the original data to the mean values of primed hPSCs (for human cells) or mouse ES cells (for mouse cells) in each study.

For subsequent analysis of gene expression, genes were retained in both datasets if they were expressed in at least one sample, using an RPKM/FPKM > 5 threshold. Differentially expressed (DE) genes were detected by the package DESeq2 in the R software. An adjusted p value < 0.05 and an absolute value of the $\log_2$ ratio > 1 were used as the threshold for declaring gene expression differences as being significant. For the gene ontology analysis of the DE genes, gene lists were subjected to DAVID bioinformatics tool. Terms that had a P value of less than 0.05 were defined as being significantly enriched.

Principal components analysis was performed using princomp function in the R stats package based on the covariance matrix. To reduce the technical differences caused by different experiments and platforms as described above, Log2 expression values were normalized to mES cells (for mouse cells) or primed hPSCs (for human cells) in each study. Heatmaps were generated using pheatmap package in the R software. RNA-seq data were deposited in the Gene Expression Omnibus under the series accession number GSE89303.

ChIP and Sequencing Library Preparation

For each sample, approximately $5*10^6$ cells were cross-linked in PBS containing 1% formaldehyde at room temperature for 10 min, and quenched with glycine for 5 min. The fixed cells were washed twice with cold PBS, centrifuged at 20 xg and 4°C for 3 min to remove the supernatant. Cell pellets were re-suspended in hypotonic buffer (20 mM HEPES at pH 7.9, 10 mM KCl, 1 mM EDTA, 10% glycerol, 0.2% NP-40) with protease inhibitors - and incubated in ice for 20 min, and then homogenized with glass dounce for 10-20 times. The homogenates were further lysed with nuclear lysis buffer (1% SDS, 10 mM EDTA, 50 mM Tris-HCl at pH 8.0). Lysates were re-suspended in ChIP dilution buffer (0.01% SDS, 1% Triton X-100, 2 mM EDTA, 20 mM Tris-HCl at pH 8.0, 150 mM NaCl) and sonicated using Qsonica Q700 at 4°C. The size of sonicated fragments ranged between 200-500 bp. After sonication, Triton X-100 was added at the final concentration of 1% before further centrifugation. Sonicated lysates were centrifuged at 20,000 xg for 20 min at 4°C, and the supernatants were kept as the crude chromatin. Resulting chromatins were precleared with Magnetic Protein-G beads prewashed with sterile PBS/1% BSA three times for 1 hr at 4°C, and then collected by Magnetic Stand. Cleared chromatins were incubated with 2.5 μg antibody overnight at 4°C. Meanwhile, protein G beads were blocked with PBS/1% BSA. Blocked beads were collected and added to the chromatin-antibody mixture, and then incubated at 4°C for 6 hr. Chromatin-antibody-beads were washed 3 times with low salt buffer (0.1% deoxycholate, 2 mM EDTA, 50 mM HEPES at pH 7.5, 150 mM NaCl) and twice with TE (10 mM Tris-HCl at pH8.0, 1 mM EDTA) and then eluted in ChIP Elution buffer (50 mM Tris-HCl at pH 8.0, 10 mM EDTA, 1% SDS) at 70°C overnight. Eluates were treated with proteinase K (Sigma-Aldrich, P2308) at 55°C for 6 hr. DNAs were purified using QIAGEN Qiaquick PCR purification kit. ChIP-Seq libraries were prepared using the NEBNext® Ultra DNA Library Prep Kit for Illumina and sequenced using the HiSeq 2500 system (Illumina). The antibodies used were as follows: anti-H3K4me3 (5 μg, Millipore, 07-473) and anti-H3K27me3 (5 μg, Millipore, 07-449). ChIP-seq data were deposited in the Gene Expression Omnibus under the series accession number GSE89303.

ChIP-Seq Data Analysis

Human and mouse ChIP-seq reads were aligned to the human genome build hg19 and mouse genome build mm9 using the bwa (v0.7.12) (Li and Durbin, 2009) software respectively. Duplicate PCR reads were removed using Picard (version 2.6) from the aligned sequences. Chromatin profiles were calculated over all RefSeq genes and plotted using the ngsplot software. Genes that are under GO term "Developmental process" were defined as developmental genes. According to this standard, 5,760 human developmental genes and 5,819 mouse developmental genes were selected out. Concrete examples of genes were processed and visualized using the FillTrack tool of EaSeq software. MACS (version 2.10) was used to identify regions of histone marks enrichment over background with the "—broad" option.

Western Blot

Whole-cell protein extracts were isolated from primed hPSCs, hEPS, mES and mEPS cells using RIPA lysis buffer (Beyotime Technology Technology, P0013B) supplemented with protease inhibitor cocktail (Thermo Fisher Scientific, 78443) and phosphatase inhibitor cocktail (Thermo Fisher Scientific, 78428). Blots were incubated in 2% BSA/TBST at room temperature for 1 hr, and then,

they were incubated with the following antibodies in 5% BSA or 5% skimmed milk powder/TBST at 4°C overnight. For detecting MAPK pathways, the same antibodies were used for human and mouse cells: anti-ERK1/2 (1:1,000; Beyotime Technology, AM076), anti-p-ERK1/2 (1:1,000; Beyotime Technology, AM071), anti-JNK (1:1,000; Beyotime Technology, AJ518), anti-p-JNK (1:1,000; Beyotime Technology, AM516), anti-p38 (1:1,000; Cell Signaling Technology, 9212), anti-p-p38 (1:1,000; Cell Signaling Technology, 9215) and anti-β-ACTIN (1:2,000; Sigma-Aldrich, A1978). For mouse cells, the anti-PARP1 (1:1,000; Santa Cruz, sc-7150) antibody was used. Secondary antibodies were anti-rabbit IgG, HRP-linked antibody (1:5,000; Cell Signaling Technology, 7074) and anti-mouse IgG, HRP-linked antibody (1:5,000; Cell Signaling Technology, 7076), which were incubated 1 hr at room temperature while shaking. The blots were developed using BeyoECL Plus (Beyotime Technology, P0018A).

Quantitative PCR Analysis

The total RNAs from an entire well of cultured cells was isolated using the RNeasy Mini Kit. RNA was converted to cDNA using TransScript First-Strand cDNA Synthesis SuperMix (TransGen Biotech, AT301). PCR was conducted using Power SYBR® Green PCR Master Mix (Applied Biosystems, 4367659) on an ABI Prism 7300 Sequence Detection System. The data were analyzed using the delta-delta CT method. The primers that were used for real-time PCR are listed in Table S7.

Genomic PCR and Human Mitochondrial PCR Assay

Total DNA of cells, embryos and placentas was isolated using the DNeasy Blood & Tissue Kit (QIAGEN, 69506). Genomic PCR was performed using EasyTaq PCR SuperMix (Transgen Biotech, AS111). For detecting human specific mitochondrial DNA element by Q-PCR, 70 ng of total DNA per sample was used. The data were analyzed using the delta-delta CT method, which were first normalized to the values of human-mouse conserved mitochondrial DNA element. Then the relative expression values were further normalized to the values generated from control samples isolated from un-injected wild-type mouse tissues. The primers used for genomic PCR are listed in Table S7.

mRNA Detection of Human-Specific Lineage Markers

E6.5-7.5 hEPS-chimerized mouse conceptuses were isolated and homogenized using Bioruptor. Then total RNAs were extracted using Trizol. cDNA was prepared and amplified using the Smart-seq2 approach. The amplified cDNA product was diluted tenfold as required by the Q-PCR template. Quantitative PCR analysis was conducted using the KAPA SYBR FAST qPCR Kit on a Bio RAD CFX Connect Real-Time System. The primers used are listed in Table S7. To identify positive chimeric samples, the expression of human *β-ACTIN* were first analyzed. Compared to the wild-type controls, the expression of human *β-ACTIN* with an average Ct value that is at least 5 cycles less than the controls were identified as positive detection of human *β-ACTIN* expression in chimeric samples, and these samples were selected as samples with human cell chimerism. Then the expression of different human lineage markers were analyzed in these samples. Human lineage markers with an average Ct value that is at least 5 cycles less than the wild-type controls were identified as expressed markers in the chimeric samples. The positive expression of human lineage markers in chimeric samples were further examined by gel electrophoresis of Q-PCR or RT-PCR products using 2% agarose gels. The primers used for genomic PCR are listed in Table S7.

Generation of Parp1 Knockout mEPS Cell Lines

Guide RNA sequences were cloned into the plasmid px330 (Addgene, 42230). Px330 containing *Parp1* gRNAs were co-transfected into digested single mEPS cells by nucleofection (4D-Nucleofector System, Lonza). Single colonies were picked and expanded individually. Genomic DNA of colonies were extracted using the DNeasy Blood & Tissue Kit, which was further analyzed by genomic PCR. Colonies with the deletion of exon 1 and exon 2 of *Parp1* locus were identified. *Parp1* knockout mEPS cells (*Parp1*-KO) were cultured in LCDM condition without MiH (-MiH).

Tetraploid Complementation

To perform tetraploid blastocyst complementation, tetraploid embryos were first produced by the electrofusion of 2-cell stage embryos collected from mated female F1 mice, which were hybrided using male DBA2 mouse and female C57 mouse. The produced tetraploid embryos were cultured in KSOM medium in vitro to reach blastocyst stage. The genetic background of used mEPS cell lines were hybrids between C57 and 129. For the generation of tetraploid mice by multiple mEPS cell injection, 10 to 15 mouse EPS cells were subsequently injected into the cavity of each tetraploid blastocysts. For the generation of single-mEPS-derived tetraploid mice, only one mouse EPS cell was injected into the cavity of each tetraploid blastocysts. The tetraploid complemented embryos were cultured in KSOM for 2–3 hr after injection for brief recovering and then transplanted into the oviducts of pseudo-pregnant ICR mice.

Determination of the SSLP by PCR

Sequences for the primer pair were found on the Mouse Genome Informatics website (http://www.informatics.jax.org/). Genomic DNAs were extracted from tail tips of the mouse or cell pellet in culture using the DNeasy Blood & Tissue Kit, and typed using genomic PCR. Products were separated by 2% agarose gels and visualized by ethidium bromide staining.

QUANTIFICATION AND STATISTICAL ANALYSIS

Statistical Analysis

All values are depicted as mean ± SEM. Statistical parameters including statistical analysis, statistical significance, and n value are reported in the Figure legends and Supplementary Figure legends. Statistical analyses were performed using Prism Software (GraphPad). For statistical comparison, one-way ANOVA was employed. A value of $p < 0.05$ was considered significant.

DATA AND SOFTWARE AVAILABILITY

Data Resources

The accession number for the sequencing data reported in this paper is NCBI GEO: GSE89303. This parent directory includes the following datasets: GEO: GSE80732 (RNA-seq) and GEO: GSE89301 (ChIP-seq).

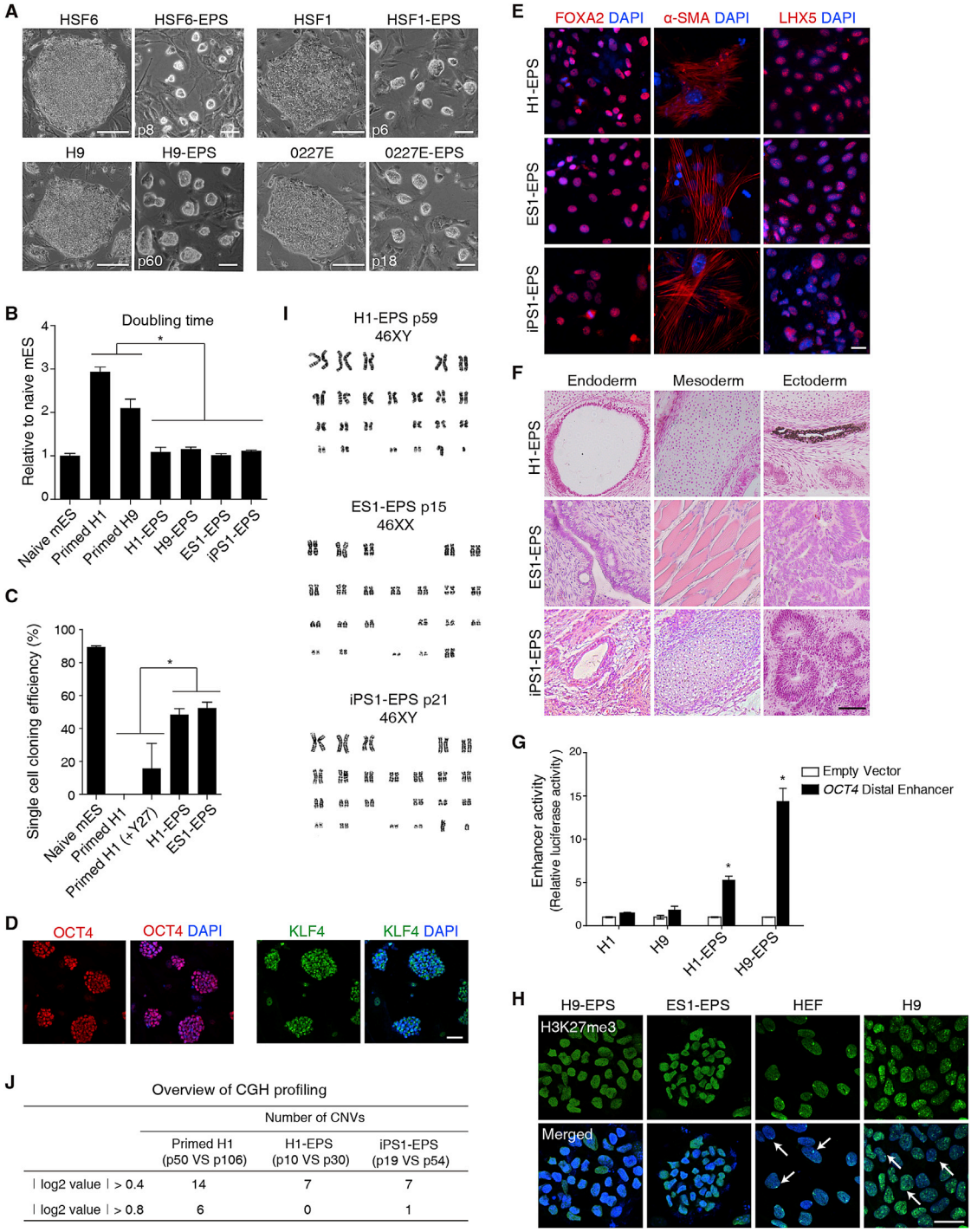

J

Overview of CGH profiling

	Number of CNVs		
	Primed H1 (p50 VS p106)	H1-EPS (p10 VS p30)	iPS1-EPS (p19 VS p54)
| log2 value | > 0.4	14	7	7
| log2 value | > 0.8	6	0	1

Figure S1. Further Characterization of hEPS Cells, Related to Figure 1

(A) Morphology of hPSC colonies before and after conversion using the LCDM condition. Scale bars, 100 μm. Similar results were obtained in at least 2 independent experiments.

(B) Population doubling time of hEPS cells, primed hPSCs and naive mES cells. Values were normalized to that in mES cells. Error bars indicate SEM (n = 3). Significant differences between values of primed hPSCs and hEPS cells were found by One-way ANOVA (*p < 0.05).

(C) Single cell cloning efficiency of different PSC types. Y27: Rock inhibitor Y27632 (10 μM). Error bars indicate SEM (n = 3). Significant differences between values of hEPS cells and primed hPSCs were found by One-way ANOVA (*p < 0.05).

(D) Immunostaining of representative pluripotent markers in hEPS cells. Scale bar, 50 μm. Similar results were obtained in at least 2 independent experiments. The pseudo-colors were used.

(legend continued on next page)

(E and F) In vitro EB differentiation (E, scale bar, 20 μm) and in vivo teratoma formation (F, scale bar, 100 μm) of hEPS cells with different origins. For each cell line, similar results were obtained in two independent experiments. For (E), the pseudo-colors were used.

(G) Predominant utilization of *OCT4* distal enhancer element in hEPS cells. Primed hPSCs were used as controls. Human *OCT4* transcriptional regulation is evaluated by the activity of distal enhancer reporter gene using the luciferase reporter assay in the indicated cell lines. Baseline activity was analyzed by transfection with an empty vector. Error bars indicate SEM (n = 3). Values were compared with that in samples transfected with the empty vector using One-way ANOVA. *$p < 0.05$.

(H) Representative confocal images obtained after immunostaining for H3K27me3 in female hEPS cells. Primed H9 cells and human embryonic fibroblasts (HEF) were used as controls. White arrows, H3K27me3 loci. Scale bar, 30 μm. For each cell line, similar results were obtained in two independent experiments.

(I) Karyotype analysis of H1-EPS, ES1-EPS and iPS1-EPS cells. The passage number at which the cells were collected for karyotype analysis is indicated. For each cell line, similar results were obtained in two independent experiments.

(J) CNVs in hEPS cells and primed hPSCs analyzed by CGH profiling. Genomic DNA from primed H1, H1-EPS and iPS1-EPS cells at early passages were used as references.

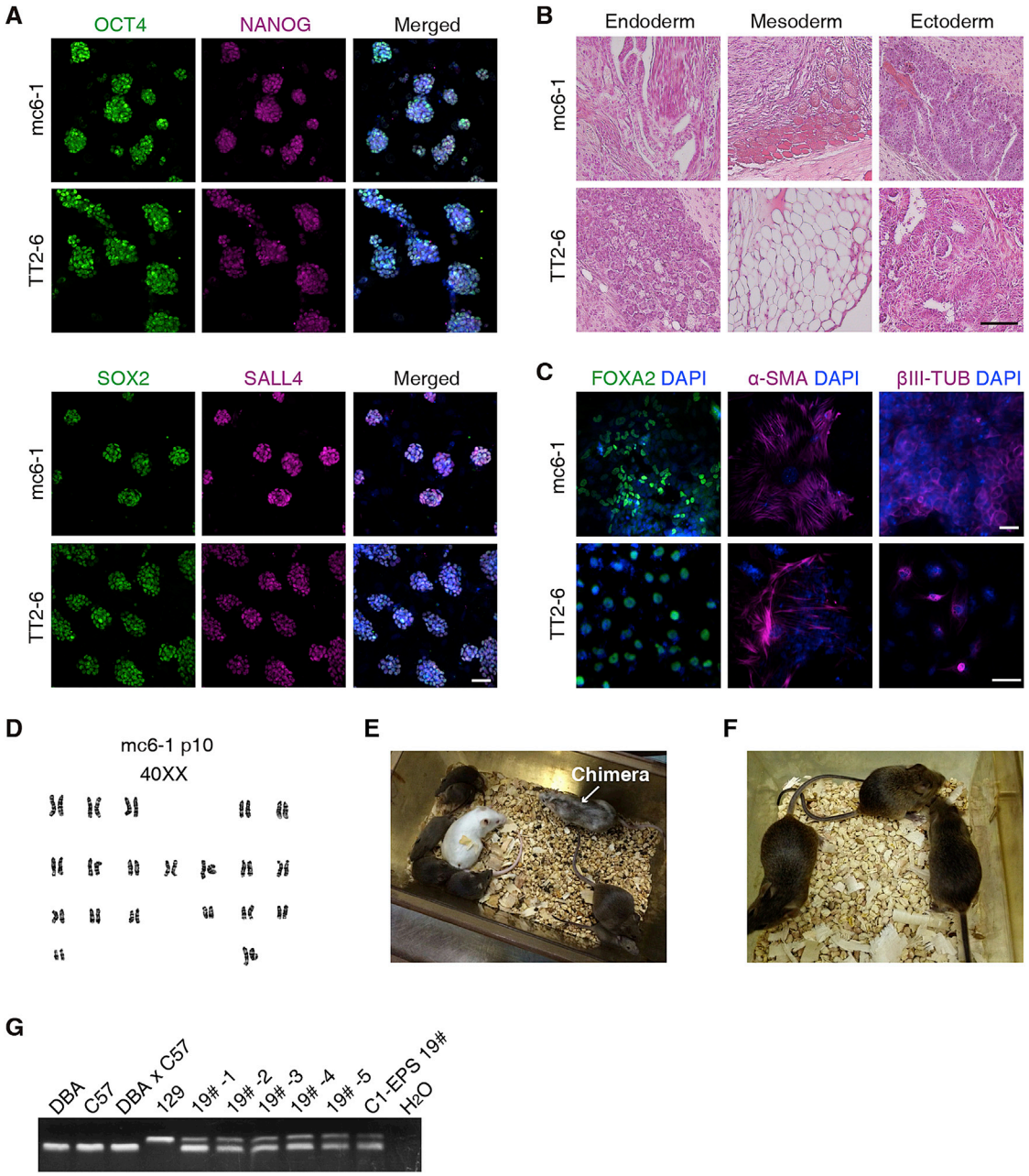

Figure S2. Further Characterization of mEPS Cells, Related to Figure 2

(A) Immunostaining of pluripotency marker gene expression in mEPS cells. Scale bar, 50 μm. Similar results were obtained in at least 2 independent experiments. The pseudo-colors were used.

(B and C) In vivo teratoma formation (B, scale bar, 100 μm) and in vitro EB differentiation (C, scale bars, 20 μm) of mEPS cells. For each cell line, similar results were obtained in two independent experiments. For (C), the pseudo-colors were used.

(D) Representative result of karyotype analysis in mEPS cells. The passage number at which cells were collected for the karyotype analysis is indicated. Similar results were obtained in two independent experiments.

(E) A representative image of the multiple mEPS cell-derived chimera and its offspring with germline transmission. Similar results were obtained in at least 2 independent experiments.

(F and G) A representative image of mEPS cell-derived mice through tetraploid complementation (F) and SSLP analysis for lineage identification (G). The polymorphic pattern of 4N mice (1# - 5#) is identical to that of the parental C1-EPS 19# cells (C57 X 129 F1 hybrid), and distinct from that of the donor of tetraploid blastocysts (hybrids generated using male DBA mouse and female C57 mouse).

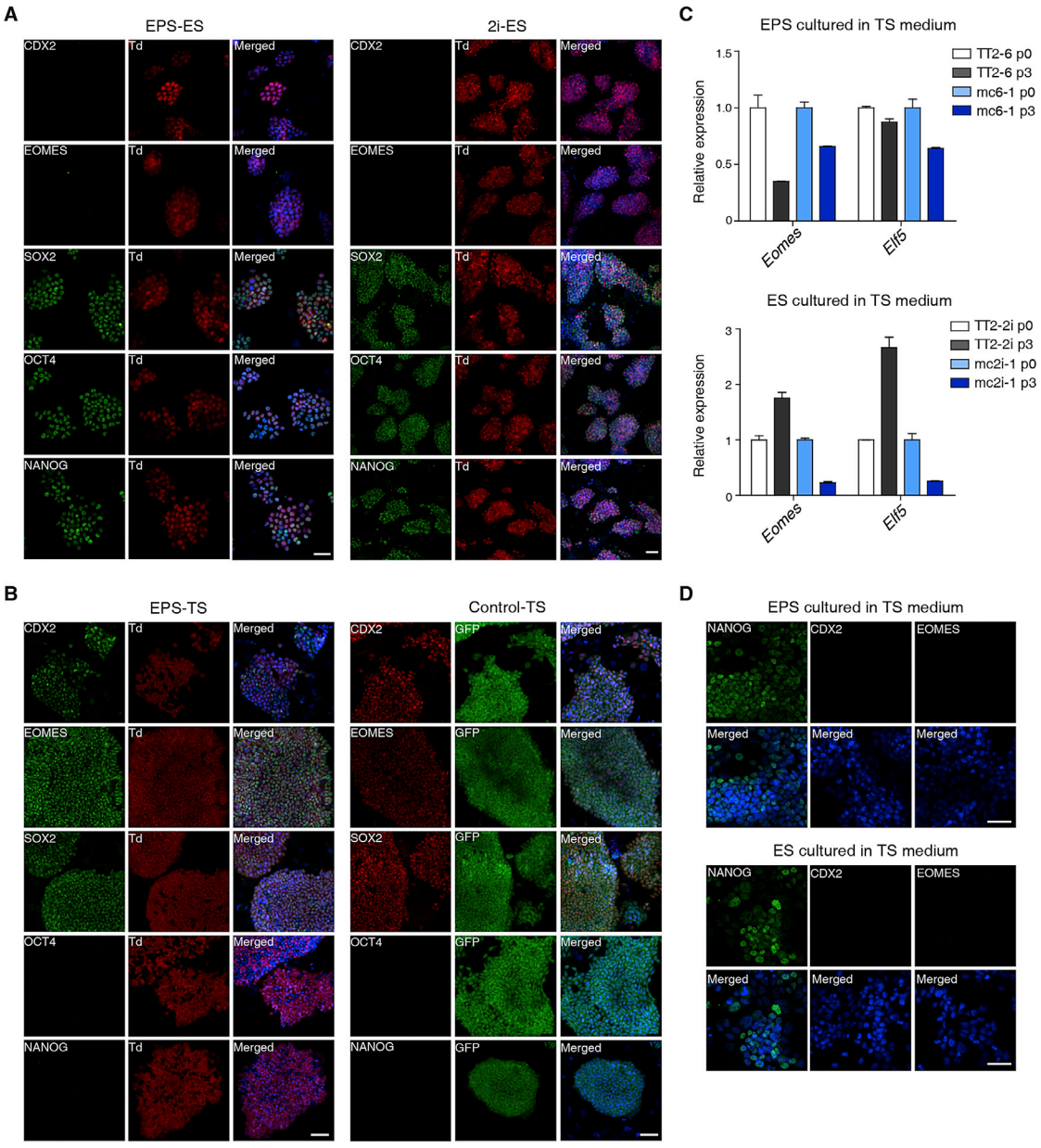

Figure S3. Further Analyses of mEPS-Derived ES and TS Cells, Related to Figure 3

(A and B) Representative images of immunostaining of ES and TS markers in EPS-ES (A, left panels), 2i-ES cells (A, right panels), EPS-TS (B, left panels) and control of GFP labeled-TS cells (B, right panels). Td: Tdtomato fluorescent signal. GFP: GFP fluorescent signal. Scale bars, 50 μm. Similar results were obtained in at least 2 independent experiments. The pseudo-colors were used.

(C) Relative expression of representative TS marker genes in cells cultured in conventional TS medium. mEPS cells cultured in LCDM condition (TT2-6 p0 and mc6-1 p0) or mES cells cultured in 2i condition (TT2-2i p0 and mc2i-1 p0) were used as controls respectively. Error bars indicate SEM (n = 2). Similar results were obtained in at least 2 independent experiments.

(D) Immunostaining of ES and TS marker genes in EPS cells (upper images) or ES cells (lower images) cultured in TS medium. Scale bars, 50 μm. Similar results were obtained in at least 2 independent experiments.

A

Percentage of single-cell chimerism

	Embryo	Yolk sac	Placenta
1#	62.7%	36.2%	7.76%
2#	28.0%	25.9%	5.4%
3#	17.8%	16.9%	2.41%
4#	21.5%	25.6%	3.45%
5#	71.2%	60.4%	13.0%

C

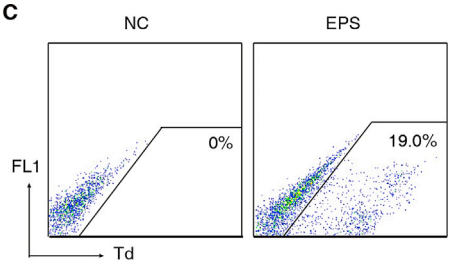

Placenta	%
1#	1.05
2#	1.09
3#	1.17
4#	1.68
5#	1.84
6#	6.09
7#	10.8
8#	19.0

B

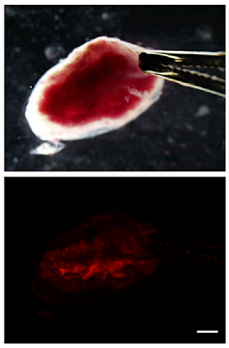

D

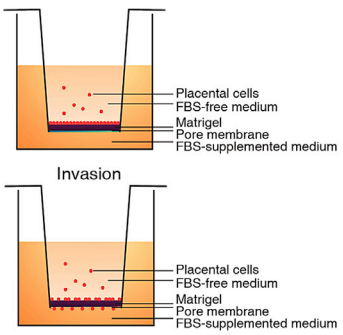

G

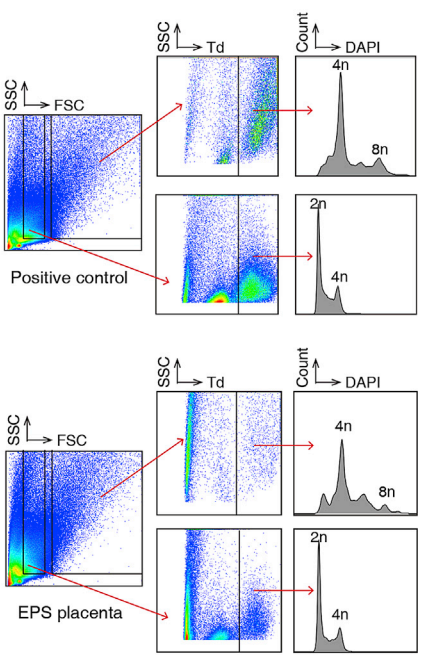

E

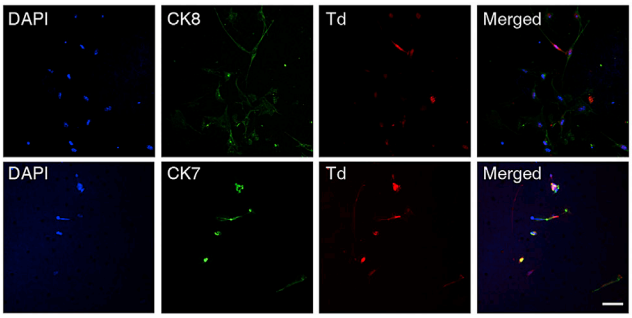

F

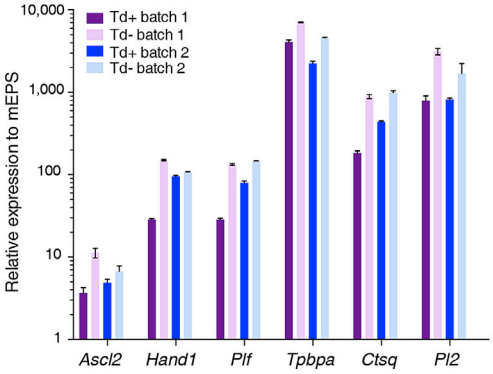

H

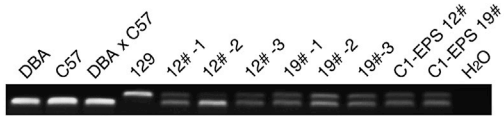

I

Summary of production
of single EPS-derived mice by tetraploid complementation

Cell lines	Injected 4N blastocyst*	Born pups	Live pups
C1-EPS 12#	140	3	3
C1-EPS 19#	171	4	1

*: 4N embryos were produced by the electrofusion of 2-cell stage embryos collected from mated female F1 mice, which were generated using male DBA mice and female C57 mice.

Figure S4. Single mEPS-Cell Derivations Can Contribute to Both Embryonic And Extraembryonic Parts In Vivo, Related to Figure 4

(A) Summary of FACS analysis of the percentages of single mEPS-derived cells in the E10.5 chimeric conceptuses.

(B) Representative images showing contribution of single mEPS-derived cells (Tdtomato labeled) into placenta in E17.5 mouse conceptuses from the sagittal side. Scale bar, 2.5 mm.

(C) FACS analysis of the percentages of single mEPS-derived cells in the E17.5 chimeric placentas. NC, a placenta from the non-chimeric conceptus.

(legend continued on next page)

(D and E) Representative images of the analysis of the invasive properties of chimeric trophoblast-like cells, which were isolated from the E17.5 chimeric placenta and analyzed using the transwell-based invasive assay. (D) Schematic diagram of the transwell-based invasive assay. (E) The cells that could pass through the matrigel layer and the membrane pores were immunostained with the trophoblast markers CK8 (upper panels) and CK7 (lower panels). Td: Tdtomato fluorescent signal. Scale bar, 50 μm. Similar results were obtained in at least 2 independent experiments.

(F) Expression of trophoblast marker genes in mEPS-derived cells in the E17.5 placental tissues. Two batches of samples were analyzed. Tdtomato positive (Td+) and negative (Td-) cells were purified using FACS. The expression of trophoblast markers in these cells were analyzed and normalized to that in the original EPS cells (TT2-6). Error bars indicate SEM (n = 2).

(G) FACS analysis of the DNA contents of mEPS chimeric placental cells. E10.5 placental cells from F1 hybrids between Tdtomato transgenic male and ICR wild-type female mice were used as the positive control. Placental cells were first gated into two populations basing on their cell sizes as judged by FSC values. Tdtomato (Td)-positive cells were further gated for assessing DNA contents as judged by the intensity of DAPI signals. Similar results were obtained in at least two independent experiments.

(H) SSLP analysis for lineage identification of the single mEPS cell-derived mice through tetraploid complementation. The polymorphic pattern of 4N mice (12#-1, 12#-2, 12#-3, 19#-1, 19#-2 and 19#-3) is identical to that of the parental C1-EPS 12# or C1-EPS 19# cells (C57 X 129 F1 hybrids), and distinct from that of the donor of tetraploid blastocysts (hybrids using male DBA mouse and female C57 mouse).

(I) Summary of tetraploid complementation by single-mEPS-cell injection assay.

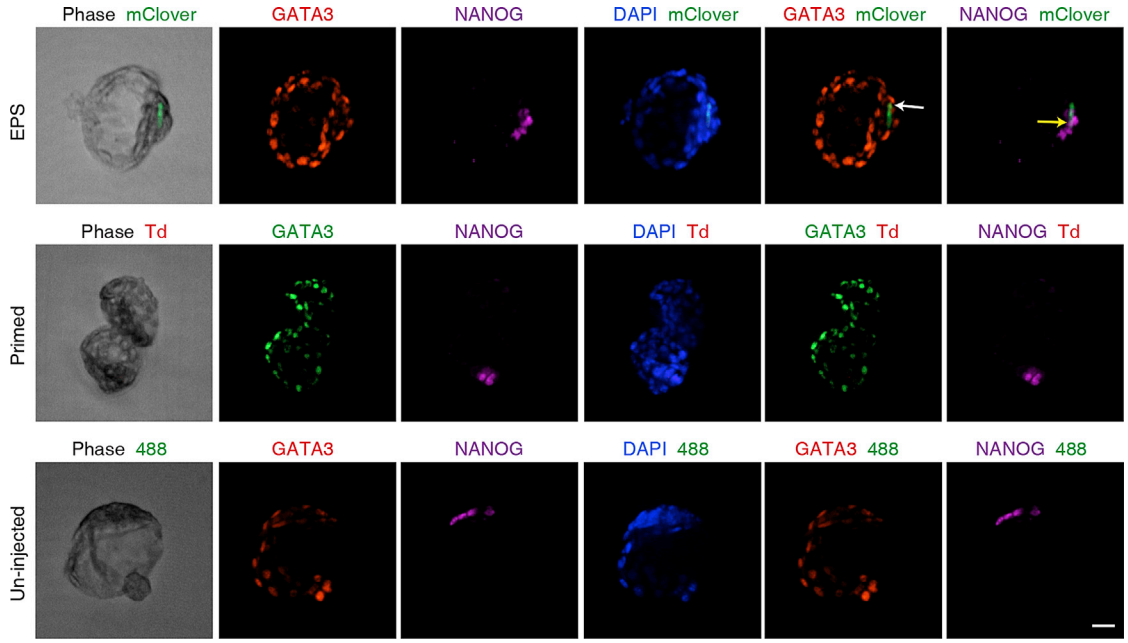

Figure S5. A Single hEPS Cell Can Chimerize Both ICM and TE Lineages in Human-Mouse Interspecies Chimeric Blastocysts, Related to Figure 5

A single mClover-labeled hEPS cell was microinjected into one mouse 8-cell embryo, and the injected embryo was cultured for an additional 48-60 hr. Then, the embryos were co-immunostained with anti-GATA3 and anti-NANOG antibodies. Tdtomato-labeled primed hPSCs were used as controls. mClover: direct observation of mClover fluorescent signal. Td: direct observation of Tdtomato fluorescent signal. 488: fluorescent signal from the 488 channel. White arrow, $mClover^{+}/GATA3^{+}$ cells; Yellow arrow, $mClover^{+}/NANOG^{+}$ cells. Scale bar, 20 μm. Similar results were obtained in at least two independent experiments.

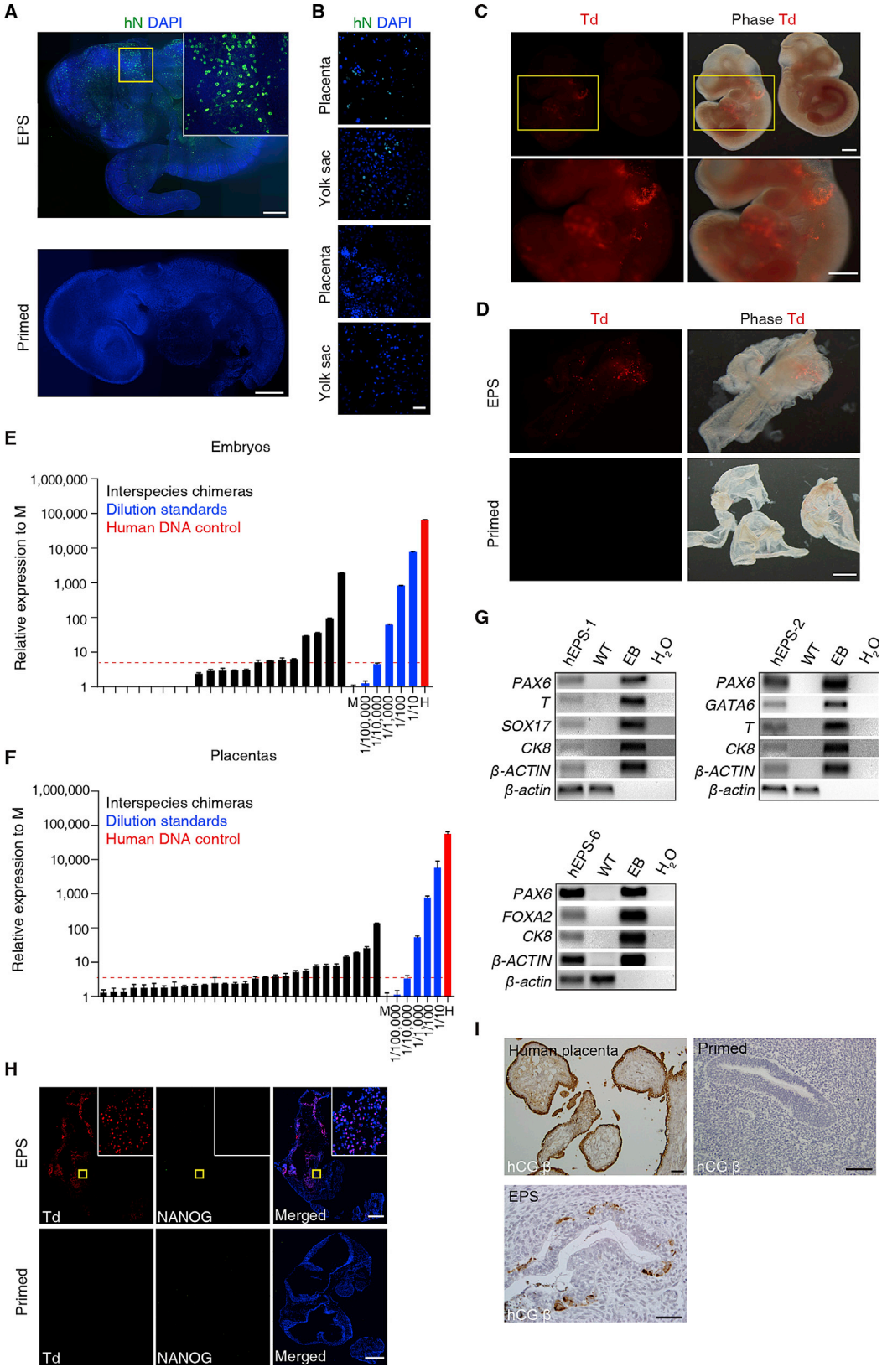

(legend on next page)

Figure S6. hEPS Cells Integrate into Both Embryonic and Extraembryonic Tissues in Human-Mouse Interspecies Chimeric Conceptuses, Related to Figure 6

(A) Representative whole-embryo images of E10.5 embryos injected with hEPS cells (upper image, 12 focal-planes) or primed hPSCs (lower image, 17 focal-planes) (z stack interval 10 μm and stitch from the XY stage ROI with a 10% overlap using "UltraVIEW XY stage") after immunostaining with the anti-human nuclei (hN) antibody. The insets are enlargements of the yellow boxes. Scale bars, 350 μm. Similar results were obtained in at least 2 independent experiments.

(B) Representative images of primary cells which were isolated from placenta or yolk sac separately from the same E10.5 conceptus as that in panels (A). The conceptuses were injected with hEPS cells (2 upper images) or primed hPSCs (2 lower images). The cells were analyzed by confocal immunofluorescence after being immunostained with an hN antibody. Scale bar, 20 μm. Similar results were obtained in at least 2 independent experiments.

(C) Representative images showing E10.5 embryos isolated from mouse conceptuses injected with Tdtomato-labeled hEPS cells. Td: Direct observation of Tdtomato fluorescent signal. Upper panels: embryo shown on the right side is from an un-injected mouse conceptuse. The lower panels were enlargements of the yellow boxes in the upper panels. Scale bars, 1 mm. Similar results were obtained in at least 2 independent experiments.

(D) Representative images showing E10.5 yolk sacs isolated from mouse conceptuses injected with Tdtomato-labeled hEPS cells, or primed hPSCs separately. Td: Direct observation of Tdtomato fluorescent signal. Scale bar, 1 mm. Similar results were obtained in at least 2 independent experiments.

(E and F) Quantitative PCR analysis for human mitochondrial DNA indicated the presence of human cells in mouse embryos (E) and placentas (F) at E10.5 following injection of hEPS cells at the 8-cell or blastocyst stages. A human DNA control (H, red bar) and a series of human-mouse cell dilutions (blue bars) were run in parallel to estimate the degree of human cell contribution. The dashed line indicates the detection level of human mitochondrial DNA equivalent to a dilution of 1 human cell in 10,000 mouse cells. M, mouse cells.

(G) Representative RT-PCR analysis of E6.5-E7.5 human-mouse chimeric conceptuses using human specific primers for different human lineage markers. Mouse *β-actin* and human *β-ACTIN* genes are analyzed as controls. WT: wild-type E6.5-E7.5 mouse conceptuses. EB: differentiated human cells from hPSCs by EB assay. hEPS-1, −2, −6 indicate three analyzed chimeric samples.

(H) Representative whole-embryo confocal immunofluorescent images (stich with 10% overlap using "ImageXpress Micro High Content Screening System") showing E10.5 embryos injected with Tdtomato-labeled primed hPSCs and hEPS cells, which are stained with an anti-NANOG antibody. Td: Direct observation of Tdtomato fluorescent signal. Insets are enlargements of the yellow boxes. Scale bars, 200 μm. Similar results were obtained in at least 2 independent experiments.

(I) Images of the hEPS-derived and primed hPSC-derived teratomas by immunostaining with the antibody specific to the human trophoblast marker hCGβ. Scale bars, 50 μm. Similar results were obtained in at least two independent experiments.

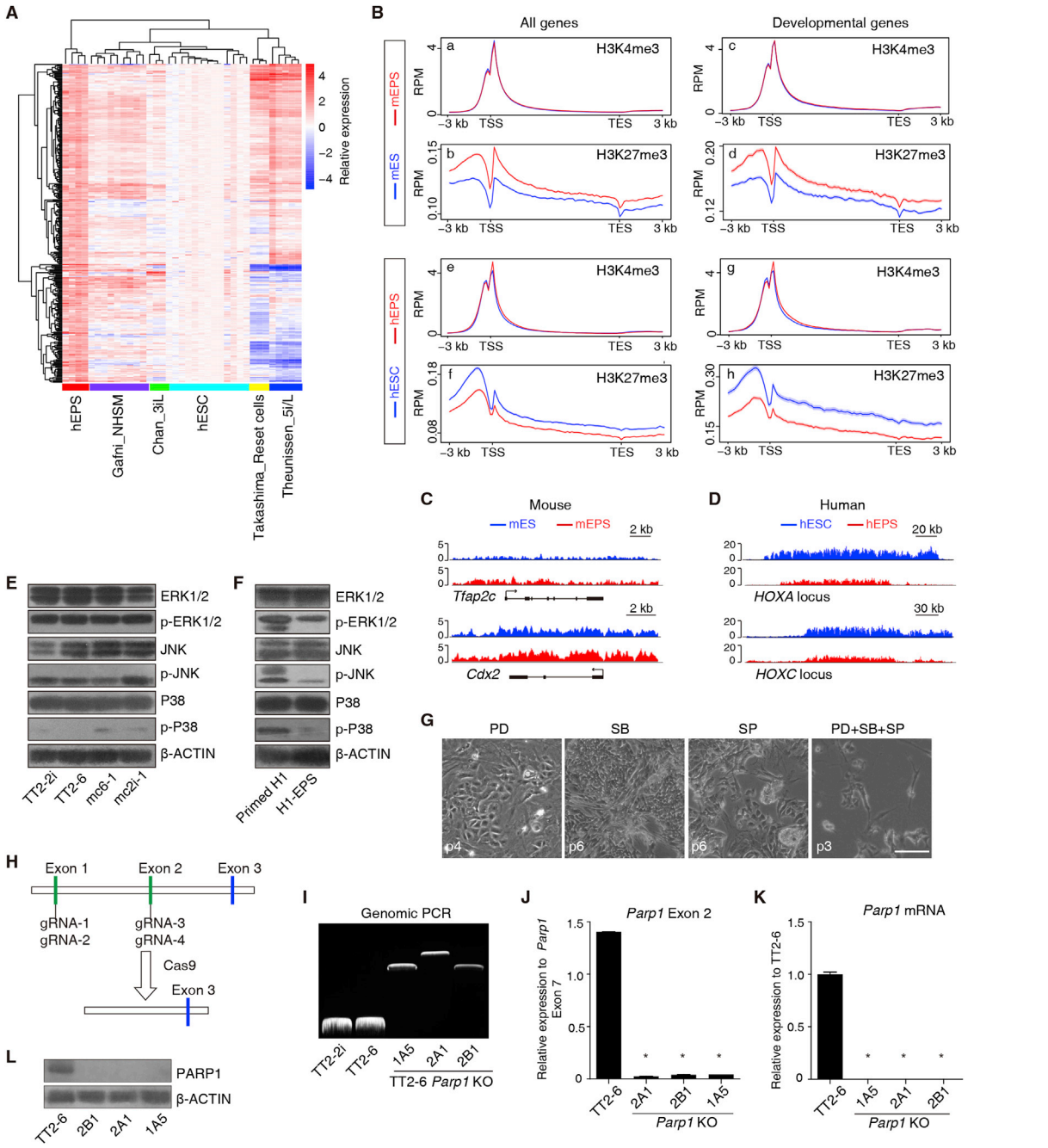

Figure S7. Further Analyses of the Molecular Features of EPS Cells and the Influence of DiM and MiH on EPS Developmental Potency, Related to Figure 7

(A) Heatmaps showing a significant portion of genes from Module C (Figure 7D) is shared among hEPS cells and naive hPSCs (Gafni (NHSM), Chan (3iL), Takashima (Reset cells), and Theunissen (5i/L)). Correlations between genes and samples were calculated using Euclidean distance (complete linkage). Log2 expression values were normalized to primed hPSCs in each study. hESC: primed hPSCs.

(B) Average H3K4me3 and H3K27me3 signals at all RefSeq genes or developmental genes in mEPS cells (mEPS: mc6-1), naive mES cells (mES: mc2i-1), hEPS cells (hEPS: H1-EPS) and primed hPSCs (hESC: H1), represented as normalized RPM values. Panel a and b: average H3K4me3 and H3K27me3 signals at all RefSeq genes in naive mES and mEPS cells. Panel c and d: average H3K4me3 and H3K27me3 signals at developmental genes in naive mES and mEPS cells. Panel e and f: average H3K4me3 and H3K27me3 signals at all RefSeq genes in primed hPSCs and hEPS cells. Panel g and h: average H3K4me3 and H3K27me3 signals at developmental genes in primed hPSCs and hEPS cells.

(C) Examples (*Tfap2c* and *Cdx2*) showing different H3K27me3 patterns at developmental genes in mEPS (mEPS: mc6-1) and naive mES cells (mES: mc2i-1).

(D) Examples (*HOXA* and *HOXC* clusters) showing different H3K27me3 patterns at developmental genes in hEPS cells (hEPS: H1-EPS) and primed hPSCs (hESC: H1).

(legend continued on next page)

(E and F) western blot analysis for the total and phosphorylated levels of the proteins involved in MAPK signaling in the mES (TT2-2i, mc2i-1) and mEPS cells (TT2-6, mc6-1) (E), and hEPS cells (H1-EPS) and primed hPSCs (Primed H1) (F).
(G) Representative images of hEPS colonies cultured in the LCM cocktail with MAPK inhibitors. Scale bar, 100 μm.
(H) Schematic showing the generation of *Parp1* knockout mEPS cell lines. gRNAs were targeted to the sequences within exon 1 and 2 in *Parp1* locus respectively, which were co-transfected into mEPS cell line TT2-6. After the expression of Cas9 protein, genomic fragments from exon 1 to exon 2 were deleted from the *Parp1* locus.
(I) Genomic PCR analysis showing that the *Parp1* locus in three sub clones (2B1, 2A1 and 1A5) of mEPS cell line TT2-6 was successfully targeted. Wild-type mES TT2-2i and mEPS TT2-6 were used as controls.
(J and K) Genomic Q-PCR and QRT-PCR analysis showing the absence of *Parp1* exon 2 fragment (J) and *Parp1* mRNA expression (K) in *Parp1* knockout mEPS sub-clones (*Parp1* KO). Wild-type mEPS cell line TT2-6 was used as the control.
(L) Western blot analysis showing the absence of PARP1 protein expression in *Parp1* knockout mEPS sub-clones (2B1, 2A1 and 1A5). Wild-type mEPS cell line TT2-6 was used as the control.
PD, PD 0325901; SB, SB 203580; SP: SP 600125.